ALBERT-LUDWIGS
UNIVERSITÄT FREIBURG

HYDROLOGIE FREIBURG

Concepts For Network Structures On Hillslopes

Julian Haas

Diplomarbeit unter Leitung von Prof. Dr. Markus Weiler
Freiburg, Oktober 2009

Albert-Ludwigs-Universität Freiburg im Breisgau
Institut für Hydrologie

Concepts For Network Structures On Hillslopes

Diplomarbeit vorgelegt von

Julian Haas

im Oktober 2009

Referent: Prof. Dr. Markus Weiler

Koreferent: Prof. Jeffrey J. McDonnell

Eidesstattliche Erklärung

Hiermit erkläre ich, dass ich diese Arbeit selbstständig und nur unter Verwendung der angegebenen Hilfsmittel angefertigt habe.

Freiburg, 20. Oktober 2009 Julian Haas

Danksagung

Zuerst möchte ich mich bei Herrn Prof. Dr. Markus Weiler für die Vergabe und Betreuung dieser Diplomarbeit und bei Herrn Prof. Jeffrey J. McDonnell für die Übernahme des Koreferats bedanken. Herrn Georg Jost und Herrn Bastian Nordmann danke ich herzlich für die freundliche Überlassung der Daten aus ihren Beregnungsexperimenten.

Meinen Eltern und meiner Schwester danke ich für die jahrelange Unterstützung, die mir dieses Studium ermöglichte, und für die Geduld und Rücksicht, die nötig ist, um eine gute Beziehung zueinander über eine räumliche Distanz zu pflegen.

Meiner WG danke ich für die Rücksicht, die sie in den Phasen des konzentrierten Arbeitens auf mich genommen haben, und für die Versorgung, wenn ich es mal wieder nicht zum Einkaufen geschafft habe.

Reule und Smoff danke ich für die anregende Kritik und die Last-Minute-Korrekturen an dieser Arbeit, meinen Kommilitonen für die schöne Zeit im Studium.

Mein aller größter Dank gilt allerdings meinem Freund Alex, ohne dessen Einsatz hier wahrscheinlich nicht eine Zeile stehen würde.

Table of Contents

List of figures

List of tables

Abstract

A major question in hydrology still is the issue of transferability of information about the hydrological feature of a hillslope or catchment to another location. Transference value of information derived from hillslope experiments remains low. Therefore it is necessary to identify the first order controls on catchment behavior to focus on these when information is transferred.

As a tool to quickly test the relevance of a certain process in a simple modeling environment virtual experiments and the model Hill-Vi were introduced.

Due to the fact that several studies pointed out that roots can be an important factor for initiation of preferential flow the relevance of root geometry on pipe flow is evaluated.

Therefor an approach to generate pipe geometries with root parameters derived from forestal literature was tested. This geometry was then used to run a model with data gained from sprinkling experiments on large plots.

A set of soil parameters was calibrated to runoff data from sprinkling experiments. These parameters were subsequently used to validate the model. Calibrations as well as validations were evaluated with focus on sensitivity of the parameters.

The simulations produced very good results in terms of model efficiency, but also showed that the data derived from literature is not sufficient in hydrologic terms and can easily be replaced by data more easily to derive.

Keywords:

Hillslope hydrology, preferential flow, virtual experiments, forest hydrology.

Zusammenfassung

Eine der größten Herausforderungen in der Hydrologie bleibt die Übertragung von Informationen über ein Einzugsgebiet in ein anderes. Der Wert dieser Informationen ist nach wie vor gering. Deshalb ist es notwendig die primären Kontrollmechanismen auf das Verhalten eines Einzugsgebietes zu ermitteln um sich auf jene beim Informationstransfer zu beschränken.

Um die Relevanz von Prozessen schnell testen zu können wurden 'Virtual Experiments' und das Modell Hill-Vi vorgestellt.

Anhand einiger Studien wurde gezeigt, dass Wurzeln zu den wichtigsten Initiatoren von präferentiellen Fließwegen zählen. Aus diesem Grund wird die Relevanz der Wurzelgeometrie auf den Fluss in Soilpipes analysiert.

Es wurde eine Methode zur Modellierung von Wurzelgeometrien anhand von Werten aus der forstlichen Literatur entwickelt. Diese Geometrie wurde dann in das Modell Hill-Vi implementiert um einige Beregnungsexperimente zu modellieren.

Bodenparameter wurden dann anhand dieser Beregnungsdaten kalibriert und anschließend zur Validierung des Modells genutzt. Dabei lag der Schwerpunkt auf der Analyse der Sensitivität der jeweiligen Parameter.

Gemessen an der Modelleffizienz ergaben die Modellierungen sehr gute Ergebnisse. Dennoch wurden aufgezeigt, dass die Daten aus der Literaturrecherche unter hydrologischen Gesichtspunkten nicht ausreichen. Das Modell könnte leicht mit einfacher zu ermittelnden Daten betrieben werden.

1. Introduction

Hillslope hydrology is considered to be stuck in a situation where advances happen slowly. Old concepts are used over and over again to parametrize more and more hillslopes, while the transfer volume from one catchment to another remains low (Weiler & McDonnell 2004).

To advance faster recent scientific approaches need to be modified to improve their captivity to identify first order processes which are worth to be considered, as well under an experimentalist's point of view as in terms of a modeler, both being essential in modern hillslope hydrology (Weiler & McDonnell 2007).

To test certain processes quickly on their relevance for a hydrologic problem conceptual models can be used (Weiler & McDonnell 2004).

Tree species is a dominant factor on soil properties and therefore on hydrologic properties. Roots make highly compacted soils accessible for infiltration (Nordmann et al. 2009) and so forests have the largest potential on soils where vertical infiltration is inhibited by compacted layers. Also the root systems of trees take the largest influence on water retention (Lüscher & Zürcher 2002). Either for economical reasons, like the need of more cheap wood for building or heating, or ecological reasons, like the changing climate some IPCC scenarios warn of, tree species on a stand might change. The change of hydrological features related to this need to be estimated.

One hydrological process related to trees is the occurrence of preferential flow along roots (Devitt & Smith 2002, Holden 2005). To estimate the change of tree species, what would also result in a change of root geometry, the relevance of root geometry needs to be determined.

2. Objectives

The aim of this study is to improve the understanding of self-organizing network structures of preferential flow on forested hillslopes.

Focus here is on the effect of pipeflow along roots and in rootchannels of two major central-European tree species, Norway Spruce and European Beech. To attain the needed data an intense review of the recent forestal literature concerning coarse root structure had to be made.

For testing this effect the model Hill-Vi, which already contains the possibility to simulate preferential flow in soil pipes, is modified to cope with more complex pipe geometries.

First a module was developed to generate a pipe geometry with the parameters of a natural root system.

The model was then calibrated and validated using data from six sprinkling experiments conducted in two separate studies. Model efficiencies and parameter sensitivities, especially of the root parameters, for the different modelings are then compared.

From this procedure answers to the following questions were expected:

- Does information about root systems ease the parametrization of hillslope models?
- Do these parameters improve the prediction of subsurface flow?
- Is the information from literature sufficient to hydrological means?

3. State of the art

3.1. Hillslope hydrology

A major question in hydrology still is the issue of transferability of information about the hydrological features of a hillslope or a catchment to another location. Transference value of information derived from hillslope experiments remains low. Especially transfer behavior of effects like soil properties and bedrock topography remains difficult despite of the knowledge about scaling effects of hillslope characteristics (Weiler & McDonnell 2004).

During the last few years a call for new approaches to this issue emerged (Weiler & McDonnell 2004). These demands were mostly inspired by the insight that the advances in hillslope hydrology after the International Hydrological Decade (IHD) somehow slowed down (Weiler & McDonnell 2007) and older approaches still stand against new approaches (Weiler & McDonnell 2004).

These deficits were ascribed to both experimentalists and modelers in hydrology. Hillslope experimentalists are criticized not to be able to even make statements about the minimal sets of measurements necessary to characterize a hillslope and to lack the ability to generalize and theorize their vast knowledge about hillslope reaction (Weiler & McDonnell 2007), while the modeler wants to incorporate small scale physics into complex models to simulate effects of larger scale (Weiler & McDonnell 2004). This lack of communication between modeler and hillslope experimentalist results in few integration of hillslopes as an important part in catchment models. Also important processes like, for example, bedrock seepage were not integrated in most hillslope models in spite of knowledge from experimentalists about its importance (van Meerveld & McDonnell 2006). This dialog between experimentalist and modeler is still considered to be out of reach. Experimentalists propose perceptual models based on field observations while modelers prefer to further incorporate physics. Therefore a basis for the dialog was tried to be established. To this use Weiler & McDonnell (2004) introduced virtual experiments. Virtual experiments are there defined as 'numerical experiments with a model driven by collective field intelligence', what means to incorporate knowledge of both experimentalist and modeler.

Virtual experiments should also serve as a tool for exploring first order controls on hillslope hydrology, since these controls are the primer effects to be transferred from one catchment to another. They should bring forth systematic examination of first order controls instead of more campaigns on new hillslopes and were the reaction to a call for a quantitative framework to test and compare first order controls instead of highly complex physically-based models since these models are often right for the wrong reason (Seibert & McDonnell 2002).

The question for first order controls is the question of how much complexity is needed in hillslope hydrology to simulate outflow and internal hillslope dynamics: Should distinct processes be included in hillslope models and how can they be conceptualized and parametrized (van Meerveld & Weiler 2008)?

Van Meerveld & Weiler (2008) showed that the inclusion of bedrock seepage improved long-term subsurface flow simulation. The same applies for hillslope topography as initiator for preferential flow (van Meerveld & McDonnell 2006).

Complex hydrological descriptions derived from field studies are difficult to implement in models due to differences in scale of the measurements and the processes modeled and the natural heterogeneity of catchments (McGuire et al. 2007). One process still poorly understood in hillslope hydrology is the effect of lateral flow like of macropores and soil pipes on the subsurface flow response and the connectivity and dynamics of the saturated zone (Sidle et al. 1995, Uchida et al. 2005, Weiler 2005, Weiler & McDonnell 2007). The conceptualization and parametrization of the effects of lateral preferential flow remains difficult (Sidle et al. 2001) and is one of the greatest challenges in hillslope hydrology, since current models often ignore such behavior (Weiler & McDonnell 2007).

3.2. Subsurface stormflow and preferential flow

Subsurface stormflow, in literature also called lateral flow, interflow or soil water flow, occurs when water moves laterally down a hillslope through soil layers or permeable bedrock, producing fast runoff components. In a humid environment and steep terrain with conductive soils, subsurface stormflow may be the main mechanism of storm runoff generation (Weiler et al. 2005).

Different concepts for subsurface stormflow were presented including transmissivity feedback, lateral flow at the soil-bedrock interface, interflow in the organic layer and pressure wave translatory flow (Weiler & McDonnell 2004, Weiler 2005).

Various studies showed that subsurface stormflow plays a crucial role in different processes and effects like stream chemistry (Uchida et al. 2001), impacts on water quality by rapid transport of fertilizers and herbicides (Gish et al. 1998) and nutrient leeching (Johnson & Lehmann 2006), and it affects landslide generation due to the creation of areas with highly positive pore pressures (Weiler 2005). The concept also helps to understand the old water paradox, which was first presented by Kirchner (2003). Invading water produces perched water tables resulting in rapid subsurface runoff and mixes with older water which is then transported quickly to the stream (McDonnell 1990). Recent intercomparison studies show, that lateral preferential flow is highly threshold dependent and occurs only after a certain amount of rain has fallen (Uchida et al. 2005).

Another process producing fast subsurface runoff is preferential flow in macropores, soil pipes and areas with higher permeability than the surrounding matrix (Weiler 2005). For better differentiation it is common sense to define vertically orientated preferential flow paths as macropores and laterally orientated flow paths as soil pipes (Faeh 1997, Weiler et al. 2003).

This process is in general deemed as important and considered to generate a vast part of the runoff during rainstorm events (Nieber & Warner 1991, Noguchi et al. 1999). Observable soil features appear to be the initiators of the majority of the preferential flow paths (Perillo et al. 1999). Macropores and soil pipes are made by subsurface erosion, especially at the surface-bedrock interface, fractures and fissures in the soil and bedrock, animal burrows and decayed or living roots. They form the basis of a ‘backbone’ for lateral subsurface flow in many sites (Beven & Germann 1982, Sidle et al. 2001).

Of these initiators the roots are the ones mentioned pretty early in publications (Beven & Germann 1982) but still remain considered in just a few works (Bonell 1993, Mitchell et al. 1995, Devitt & Smith 2002, Holden 2005). Nevertheless they are proven by dye tracing experiments (Noguchi et al. 1999) and considered as the most important initiators for preferential flow, even through areas with different soil properties (Perillo et al. 1999) and unsaturated soil (Beven & Germann 1982). Roots, as well living as dead, form macropores and pipes, which can make up at least 35 % of the volume of a forest soil (Aubertin 1971). This results in about 70 % of the pipes being formed by roots (Noguchi et al. 1999), while in soils with a low pH, like under coniferous stands, due to a lack of faunal activities, it can be up to 100 % (Hagedorn & Bundt 2002).

The processes underlying the generation of these pipes by dead roots are the erosion of the root channels (Weiler et al. 2003) on the one hand and sustaining of the bark of dead roots, forming stable hoses due to the fast decay of the xylem, on the other hand (Beven & Germann

1982). Living roots can create fissures at the soil-root interface or cause the compaction of the surrounding soil which leads to a change of the saturated hydraulic conductivity, so the infiltration on the bottom of the root channel is reduced (Oswald et al. 2008). In opposite Beven & Germann (1982) mention that new growing roots can sometime clog macropores and pipes.

Jorgensen et al. (2002) observed that 94 % of preferential flow in a clay-rich till was along root channels. But in opposite to root systems of annual plants like crops, macropores and pipes in forest soils persist for decades (Beven & Germann 1982, Hagedorn & Bundt 2002).

Pipes mostly occur above the soil-bedrock interface or above soil layer interfaces (Uchida et al. 2001). That goes along well with the assumption described below that roots follow soil layers.

Other concepts related to roots are that holes left by trees knocked-over by wind might serve as a funneling system for water to enter a pipe system of dying roots (Beven & Germann 1982). Lange et al. (2008) investigated the influence of beech, oak and spruce on soil properties. Fine root morphology there is a key factor for infiltration. But higher fine root density does not necessarily improve infiltration. Liang et al. (2007) connects the root system of trees to a double funneling effect that is responsible for differences in upslope and downslope water dynamics of a tree.

3.3. Root systems

The root systems of trees differ from the root systems of other forestal plants like shrub or grasses by a variety of features. The most significant might be the longer life, as well of the plant itself as of its roots, and the secondary growth. These two properties also define the fraction of the root mass called skeletal roots (Polomski & Kuhn 1998). The other fraction are the fine roots which tend to be rather ephemeral. Skeletal roots are defined by a diameter larger than 2 mm, while fine roots have diameters below 2 mm (Köstler 1968).

Depending on their orientation in the soil roots are classified into vertical roots and horizontal roots (Köstler 1968). Kuhr (1999) precises this classification by defining vertical roots to have an angle between 45° and 90° and horizontal roots between 0° and 45° relative to the soil surface.

Under good growing conditions each tree species develops a typical root system. These systems are grouped in three root types and shown in Figure 1.

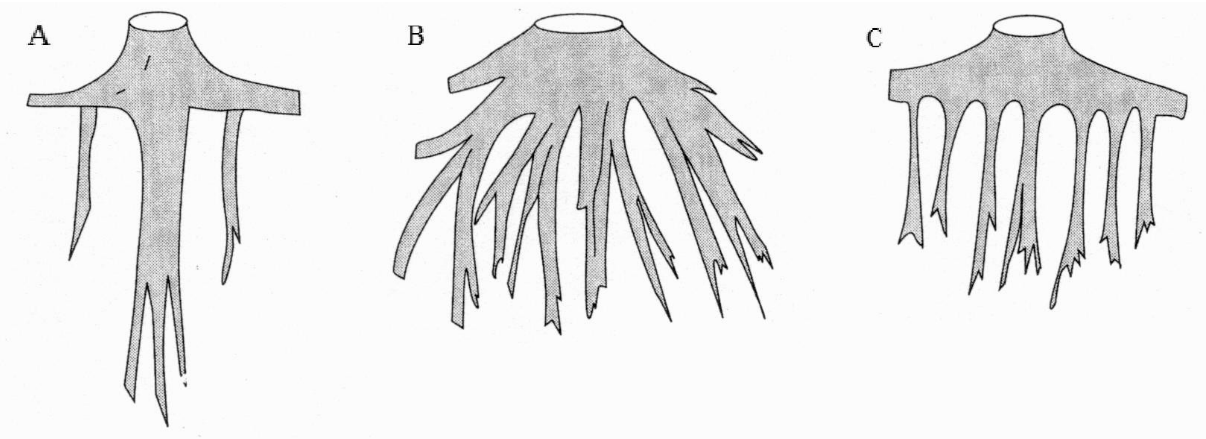

Figure 1: Root types (Polomski & Kuhn 1998)
A: Taproot system, B: heart-shaped system, C: peg root or sinker root system

The taproot system is characteristic for European Silver Fir (*Abies alba* Mill.) or Scots Pine (*Pinus Silvestris* L.). A vertically growing taproot dominates the root system. In its first years nearly every tree species has a taproot. This feature vanishes as soon as the typical system develops.

The heart-shaped system is characteristic for Douglas Fir (*Pseudotsuga menziesii* Mirb.) and European Beech (*Fagus Sylvatica* L.). The roots develop a homogeneously formed and fanning mass of braiding and branching roots. Especially in the direct vicinity to the stem this system is very dense.

The sinker root system is characteristic for Norway Spruce (*Picea Abies* Mill.) or Common Ash (*Fraxinus Excelsior* L.). The main coarse roots horizontally extend very far from the stem and close to the soil surface (Drexhage 1994). Rectangular to the main roots sinkers grow downwards (Polomski & Kuhn 1998).

During the last hundred years several studies on root systems were conducted to derive more information about the different root systems. Most of them were excavations which range from total excavations of whole root systems (Hilf 1927, Drexhage 1994, Kuhr 1999) to root counts on soil profiles. Observations are often made on plantations or on trees pulled down by machines or spontaneously for example after storms when trees are disrooted (Polomski & Kuhn 1998). Even the most extensive works don't give reliable information for statistical reasons (Kuhr 1999). Due to the lack of systematically derived data root data should in general just be considered as orientation (Polomski & Kuhn 1998).

3.4. Root parameters

Due to the sprinkling experiments described below the focus in this thesis is on two tree species: Norway Spruce (*Picea Abies* Mill.) and European Beech (*Fagus Sylvatica* L.). Also some limitations on soils can be made, since all experiments considered were conducted on stagnic cambisols. Soil and stand properties take major influence on the root systems (Friedrich 1992, Polomski & Kuhn 1998). Because of this some generalizations could be made and the focus rests on the data available for the given conditions.

Important for lateral flow are, of course, lateral roots. So another focus here is on lateral roots. Among these the coarse roots are of interest. That is because on the one hand coarse roots have enough diameter to form pipes that significantly transmit water. On the other hand fine roots are ephemeral and usually die after the vegetation period (von Gadow 2003), according to Fogel (1983) up to 86 %.

Horizontal coarse roots make up 60 to 80 % of total root mass of spruce (Köstler 1968). The main horizontal root branches of spruce are developed around the first 20 years of a tree, while the vertical roots start to significantly develop at the age of 50 and older (Kuhr 1999).

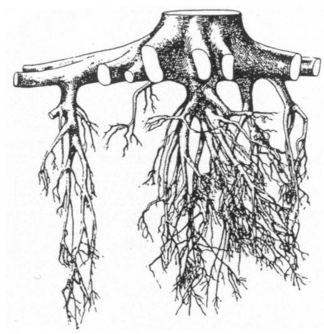

Figure 2: Sinker root system of Norway Spruce (Köstler 1968)

Figure 2 shows the root system of an adult Norway Spruce under good soil conditions. In contrast to that stands Figure 3, showing the root systems of Norway Spruce under stagnic soil conditions.

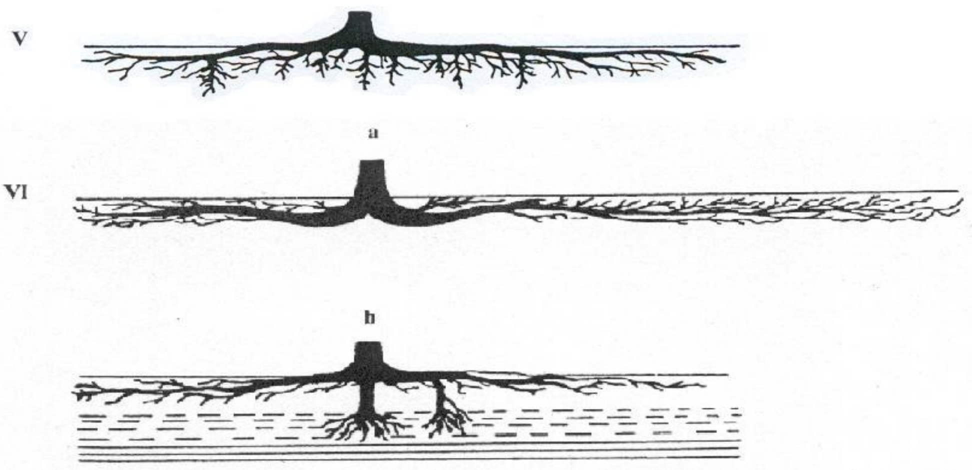

Figure 3: Norway Spruce on stagnic (V) or hydric (VI) soils

On stagnic soils or on soils with a heavily compacted layer the development of vertical roots stagnates (Figure 3: V). On soils with transient water tables or even ground water close to the soil surface the typical sinker roots do not develop at all (Figure 3: VI a). Instead fine roots rather grow laterally or upwards. Under these conditions the main coarse roots can reach extreme extensions, up to over 20 m (Polomski & Kuhn 1998). An exception is the development of single sinker roots down to the groundwater surface (Figure 3: VI b).

Beech forms the typical heart-shaped root system very early. Horizontal coarse roots, though just distinguishable as such by size, top the root body and fine roots fill the space beneath (Köstler 1968). Figure 4 shows a beech root system under good soil conditions.

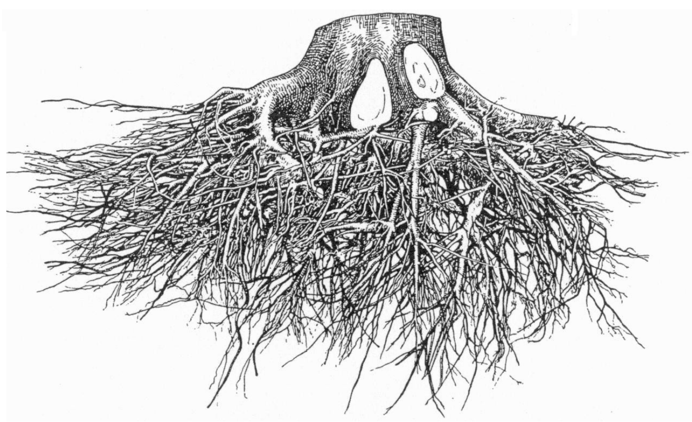

Figure 4: Root system of European Beech (Köstler 1968)

In the direct vicinity to the stem the root system is very dense. Here the largest part of the root mass is located. Still the coarse roots extend several meters.

Under stagnic conditions beech develops similarly to spruce.

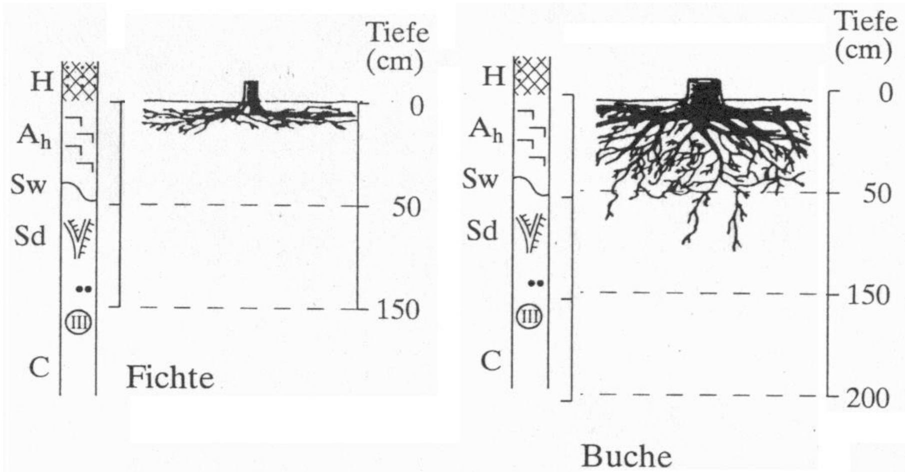

Figure 5: Spruce (left) and beech (right) on stagnic soils (Polomski & Kuhn 1998)

Figure 5 shows both tree species under stagnic soil conditions. Beech roots a little further down into the soil than spruce. But in general roots do not grow as deep as under good soil conditions and the dense system around the stem is laterally spread wider.

Polomski & Kuhn (1998) sums up facts from different studies and concludes that the best values for the root depth of coarse roots in stagnic cambisols are 30 cm to 70 cm for European Beech and 10 cm to 60 cm for Norway Spruce. Due to the lack of statistically reliable data no standard deviation is given, which makes this data just treatable as distributed uniformly. Comparing Figure 8, Figure 9 and Figure 10 it is obvious that this is not the optimal solution. The root depth distribution of beech might at least come close to uniform distribution. But for spruce a distribution with a positive skewness in favor of shallow roots would be more appropriate.

On other soils these values might differ totally. But in general Kalinin (1983) (cited in Polomski & Kuhn (1998)) states that on permeable soils roots orientate on soil layers. That includes in the first place, that on slopes, especially on rather gentle ones, roots orientate parallelly to soil surface, assuming that soil stratification is homogeneous, and in the second place, that the depth of the topsoil and root depth can correlate.

For European Beech good soil conditions have another effect. Coarse horizontal roots, though just distinguishable as such by size, top the root body and fine roots fill the space beneath (Köstler 1968). Beech then builds its root system downwards to the base of the rooted topsoil with a mean angle which can be derived by the depth of the rooted topsoil and the extension of the root system.

The best values for the extension of roots still gives Hilf (1927) with European Beech having 3.6 m of root length with a standard deviation of 1.31 m and Norway Spruce having 5.5 m of root length with a standard deviation of 2.76 m.

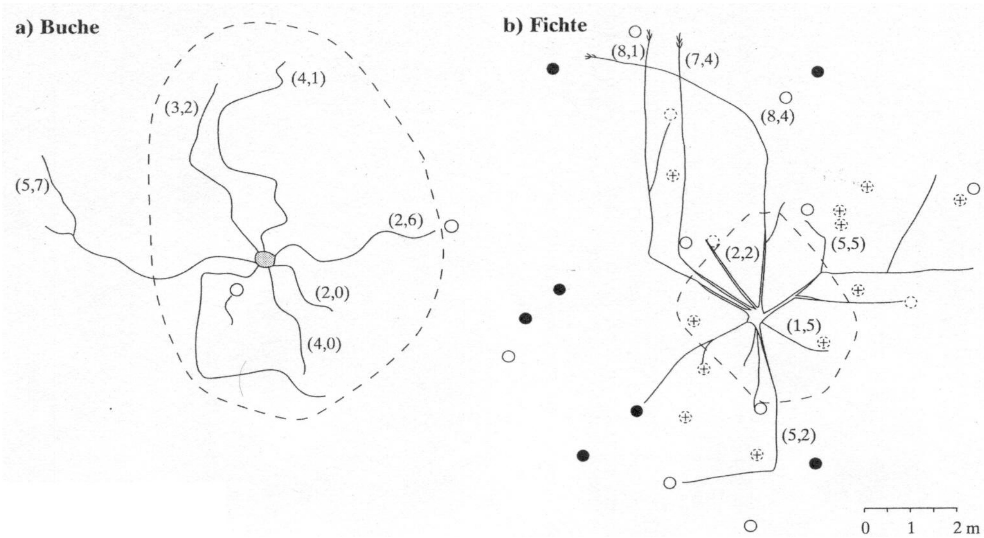

Figure 6: Extension of the root systems of European Beech (left) and Norway Spruce (right) (Polomski & Kuhn 1998)
Dashed lines show the extension of the crown. Dots are other trees. The values in parentheses is root length in m.

Figure 6 shows the extension of the main root branches relative to the crown extension for both species. Due to the lack of other data the number of main root branches is estimated from figures like this to a value of around 7. In the modeling described below this will be considered and the effect of root branch number will be tested. Anyway, coarse roots start to branch into several branches after 100 cm at the latest. But since they more or less keep their directions (Köstler 1968) they are treated as one root in the model.

4. Study Areas

The data used for modeling was derived from two sprinkling campaigns. The sprinkling campaigns were conducted and published by Jost (2004) and Nordmann et al. (2009). In the following the properties of the study areas and the plots are presented.

4.1. Kreisbach

The data published by Jost (2004) was derived from two sprinkling experiments conducted in late September 2001 on two stands with different vegetation.

The two investigated stands are located near Kreisbach in Lower Austria on around 480 m above sea level. Both stands face north with a mean angle of 20°. Mean annual precipitation is 850 mm. Mean annual temperature is 8.4°C (Schume et al. 2004).

Geologically the underlying material consists of Flysch sediments, especially sandstone and marl (Jost 2004).

The soils are stagnic cambisols. Detailed soil properties to a depth of 100 cm are given in Table 1.

Table 1: Soil data for the Kreisbach stands (Schume et al. 2004)

	Soil depth (cm)					
	10	20	40	55	75	100
Rock content (vol.%)	4	3	9	15	10	16
Bulk density (g cm^{-3})	1.17	1.19	1.30	1.24	1.39	1.44
Pore volume (%)	54	53	50	51	46	44
Clay content (grav.%)	37	56	51	44	49	56
Texture class (USDA texture triangle)	SiCL	C	C	SiC	C	C
Water content at − 1 MPa (vol.%)	18.7	18.4	19.6	18.7	23.6	25.8

Texture class is according to the Soil Texture Triangle by USDA (SiCL: Silty clay loam, SiC: Silty clay, C: Clay)

Jost (2004) observes a change in soil properties at around 60 cm of depth. This can be seen best by the change of water content at 1 MPa and the slight difference in pore volume between 55 cm and 75 cm in Table 1. Here the stagnic horizon is located. Jost (2004) expects a major part of lateral flow to happen here.

One stand is a mixture of European Beech and Norway Spruce with beech dominating by 78.1 %. On the other stand spruce dominates by 96.7 %. The mixed stand has an age of 60 years. The spruce-stand ages around 55 (Jost 2004). The dominating height of both stands was 27 m in 2000 and consisted of just one tree layer with nearly no shrub or ground vegetation (Schume et al. 2004).

Both height and age are important factors for the state of root growth. As mentioned in chapter 3.3. Kuhr (1999) states that the growth of lateral coarse roots happens to a crucial part to the age of 20. Afterwards lateral growth of coarse roots stagnates and vertical growth as well as the development of the fine root system are focused. Because of the homogeneity mentioned above the stand properties could easily be generalized and give a good setup for modeling.

4.2. Frankenwald

The sprinkling experiments published by Nordmann et al. (2009) are conducted in a subcatchment of the dam Mauthaus close to Nordhalben in Upper Franconia, Germany, called Tschirner Ködel. The catchment covers an area of 13,4 km^2 and a height from 422 to 715 m above sea level.

The climate is dominated by the cool and wet conditions of the Mittelgebirge (lower mountain ranges) in the transit zone to more oceanic continental conditions. The mean annual temperature for the period 1980-2007 is 6,7 °C. Mean annual precipitation is 1025 mm (Both according to the German Meteorological Service (Deutscher Wetterdienst) in 2008 cited in Nordmann et al. (2009)).

Geologically dominating is shale in rhythmic stratification with fine graywacke and quartzite (German: Wetzsteinquarzit) from the early Carboniferous.

There is detailed soil data available for each of the sprinkled plots in Nordmann et al. (2009). This data will be presented in the description of the plots in chapter 4.3.2.

In general the soils in the catchment are loamy cambisols with lower bulk density in the topsoils and homogeneous bulk density in the subsoil. These soil properties produce slight stagnic conditions and are thus comparable to the soils from Jost (2004).

The topsoil-subsoil interface is an aquitarde for vertical water transport. A big part of lateral waterflow might be expected here. Nordmann et al. (2009) assume the combination of uncompacted topsoils and a highly compacted periglacial base layer or the loamy remains of the parent material being essential for fast runoff generation in the Frankenwald.

In the catchment Norway Spruce is dominating by 82 %. The percentage of European Beech is 7 %. Detailed stand information is given in the plot description in chapter 4.3.2.

4.3. Plots

4.3.1. Kreisbach

From each stand a plot with 60 m² size was selected. Main criteria for the selection were comparable soil features, so the data from Table 1 applies for both plots.

The plots have a length of 10 m and a width of 6 m. To measure runoff from the sprinkling experiments described in chapter 5.1 pits were dug down to a depth of 90 cm at the downslope end of the plots covering at least the total width of the soil face. Since the width of the trenches installed was only 5 m, the actual area of the plot, for example to calculate mass balance, is just 50 m². For the measurements of soil water change a grid of TDR-sensors was installed on the plot. These soil water measurements are not subject of this work and are published in Jost (2004).

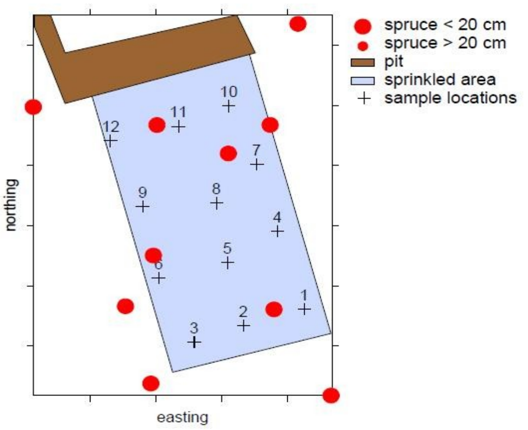

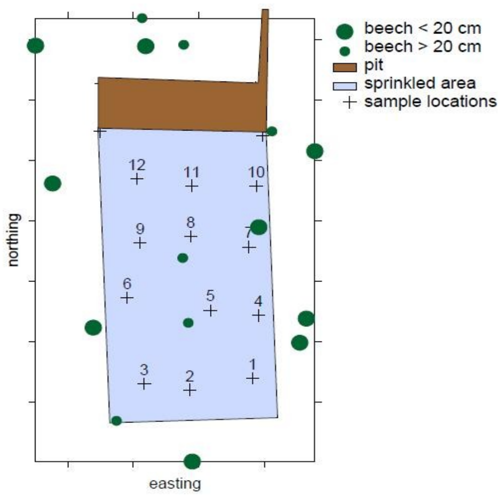

Figure 7: Sprinkled plots from the Spruce-stand (left) and the Beech-stand (right) (Jost 2004) Dots are marking the position of the particular trees.

Figure 7 shows a sketch of the two plots with dots marking the positions of the trees, the location of the pit where the trenches for runoff measurements are installed and the position of the built-in TDR-sensors.

Since the plot on the mixed stand only contains beech it is referred to as beech-plot (later B1 and B2). The other plot is referred to as spruce-plot (later S1).

4.3.2. Frankenwald

The sprinkling experiments in the Tschirner Ködel catchment considered here were conducted on three plots on two different stands. Each plot had a length of 20 m and a width of 5 m, resulting in an area of 100 m².

To get a good comparability between the two species the selected plots should have more or less similar soil properties and comparable ages of the stand. Stand properties are given in Table 2. The experiments on spruce-plots are abbreviated S2 and S3, on the beech-plots B3.

Table 2: Stand properties for the particular plots from Nordmann et al. (2009)

	Plot S2 and B3	**Plot S3**
Age of stand	103	70
Stand density (tree/ha)	337	519
Percentage of species	Beech 60/Spruce 40	Spruce 70/Beech 30
Slope	21	23
Facing	NW	NW

Despite the actual stand density given here, plots were chosen to be comparable in tree density (Nordmann et al. 2009). Due to a lack of concrete information for the definite number of trees per plot, it was set to five, which resembles the stand density of plot S3. Also it results in a better comparability to the Kreisbach plots. The spruce-plot S2 and the beech-plot B3 are in the direct vicinity to each other, only separated by a strip of 5 m of width, and belong to the same stand. The spruce-plot S3 is located separately in the catchment.

As mentioned above the soils are stagnic cambisols. Table 3 shows some general soil data for the plots. The values depicted there resemble the noticeable topsoil-subsoil interface previously interpreted as aquitard. Especially bulk density jumps to a higher value at around 60 cm of depth. Also the change of soil type is significant. Even if there is a change from rather loamy to rather sandy types, which might first lead to the unusual assumption that the subsoils have a higher conductivity than the topsoils, Nordmann et al. (2009) state that the subsoil at around 60 cm is highly compacted and therefore inhibit water flow at the interface. Another reason for this besides bulk density might be the changing content of coarse material. Since the soils overall have a high rock content the role of the material in between might be very important for soil conductivities. Furthermore the amount of fine roots, which are part of the root intensity listed in the table, raise the hydraulic conductivity as well.

Table 3: Soil properties for the Frankenwald, modified from Nordmann et al. (2009)

Plot	Depth (cm)	Soil type	Bulk density (g/cm³)	Rock content (mass %)	Coarse material (mass %)	AWC (l/m²)	Root intensity
S2	0-30	Lt2	1.07	51.1	26.7	16.1	W4
	30-60	Ls3	1.27	57.9	26.4	30.3	W3
	60-90	Sl3	1.57	57.9	18.0	53.9	W1
	90-110	Su4	1.52	67.5	10.0	70.0	W1
B3	0-30	Lt2	1.10	59.7	18.8	15.7	W3
	30-60	Lt2	1.28	49.3	30.3	30.7	W4
	60-90	Slu	1.52	61.1	19.6	54.1	W4
	90-120	Su4	1.52	76.8	9.4	70.0	W2
S3	0-30	Lt2	1.05	22.4	26.3	32.1	W4
	30-60	Lt2	1.04	41.1	29.7	52.4	W3
	60-90	Sl4	scree	75.7	16.4	60.8	W2
	90-120	Sl3	1.66	76.2	8.8	73.7	W1

Soil type is according to the Soil Triangle from DIN-Norm 4220 (Scheffer & Schachtschabel 2002): Lt=clayey loam, Ls=sandy loam, Sl=loamy sand, Su=silty sand, Slu=loamy silty sand, Sl=loamy sand. Rock content means material >20 mm. Coarse material means 2-20 mm. AWC is available water content. Root intensity is according to Bodenkundliche Kartieranleitung (Sponagel 2005): W4=heavily rooted, W3=medium intensity, W2=poorly rooted, W1=very poorly rooted.

As described in chapter 3.3. the largest amount of roots in the soil are coarse roots. This information goes well with Figure 8 and Figure 9.

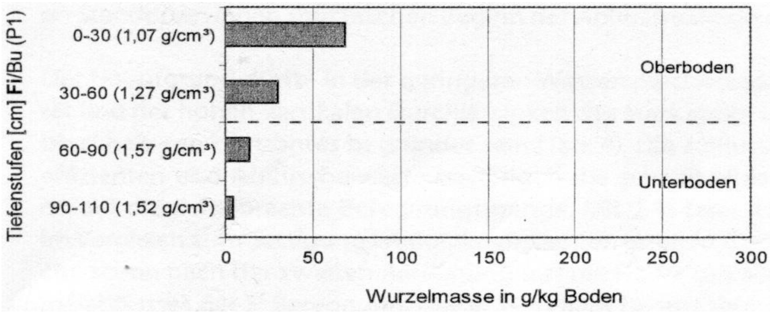

Figure 8: Soil and root properties of S2 (Nordmann et al. 2009) Ordinate is depth in cm and abscissa is root mass in g/kg soil. In parentheses after the depth values is bulk density. The dashed line is the topsoil-subsoil interface.

Each of them shows the root mass distribution with depth for one of the spruce-plots. The major part of the root mass is in the first 60 cm, where usually the lateral roots are located.

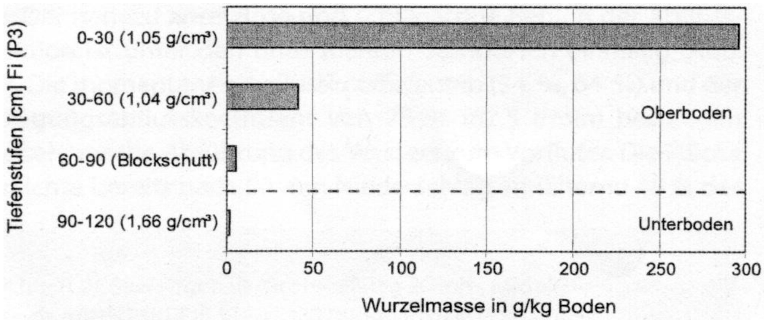

Figure 9: Soil and root properties of S3 (Nordmann et al. 2009) Ordinate is depth in cm and abscissa is root mass in g/kg soil. In parentheses after the depth values is bulk density. The dashed line is the topsoil-subsoil interface.

Figure 10 also resembles the values for beech from chapter 3.3. very well.

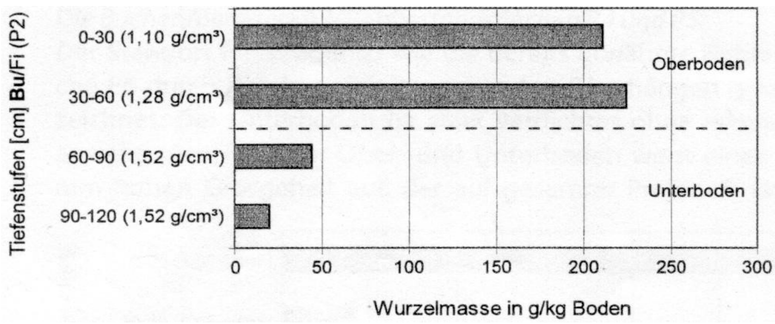

Figure 10: Soil and root properties of B3 (Nordmann et al. 2009) Ordinate is depth in cm and abscissa is root mass in g/kg soil. In parentheses after the depth values is bulk density. The dashed line is the topsoil-subsoil interface.

To measure runoff a pit was dug at the downslope end of the plot down to a depth of 2 meters and trenches were installed.

5. Methodology

5.1. Sprinkling Experiments

5.1.1. Kreisbach

For each plot two events were simulated. The first had an intensity of 100 mm/h, the second of 60 mm/h, each with a duration of one hour and a break of approximately 90 minutes in between. The precipitation generated by the sprinklers is assumed to be spatially uniform.

For runoff measurements metal sheets were built into the soil at 30 cm and 60 cm of depth and connected to trenches to get interflow data for the different levels.

During the first sprinkling on the beech-plot the lowest sheet was pushed out by water pressure. Runoff measurement was then made for the whole pit depth down to 90 cm. For modeling reasons the outflow from the different interflow levels was accumulated anyway. In the model the sprinkling experiment on the beech-plot was treated as two experiments.

In this thesis the sprinkling on the spruce-plot has the abbreviation S1 and the experiments on the beech-plot have the abbreviation B1 and B2.

5.1.2. Frankenwald

Two events were simulated, each with a duration of one hour and an intensity of 50 mm/h. Between the events a break of two hours was made. After another 2 hours' break another sprinkling with an intensity of 50 mm/h was conducted until runoff reached steady state. This took another 90 to 120 minutes. Runoff measurements went on for up to 12 hours after the start.

Again, the simulated events were assumed to be spatially uniform.

5.2. Model description

The model used for simulating the sprinkling experiments described above is the conceptual hillslope model Hill-Vi. It was first presented by Weiler & McDonnell (2004)

As mentioned above, the intention for developing Hill-Vi was to establish virtual experiments as a tool for testing different assumptions in hillslope hydrology under circumstances with no more complexity than needed. A virtual experiment needs to be able to capture all major controls on subsurface flow, an experimentalist might deem important, while at the same time being simple enough to be parametrized and understood (Weiler & McDonnell 2004).

The intention of this thesis is to test the benefit of root data, especially information on root geometry, to the prediction of subsurface flow. Therefore the model was modified with focus on the more complex routing of the flow in soilpipes resembling the architecture of the natural root system of Norway Spruce and European Beech.

5.2.1. Basic concept

The version of Hill-Vi used here is a spatially explicit and physically based conceptual hillslope model which is technically close to the version used by Weiler & McDonnell (2007).

The model is based on the concept that an unsaturated and a saturated zone defines each grid cell (Weiler & McDonnell 2006). The processes most important in this means are those controlling the water balance between the saturated and the unsaturated zone. So the primary feature of the model is to conceptualize this water balance in respect of the actual physical soil properties from field investigation (Seibert & McDonnell 2002).

The water volume in the saturated zone is according to Weiler & McDonnell (2004) given by:

$$V_{sat} = W\, A\, n_d \qquad \text{(Eq. 1)}$$

with W the water table depth (m), A the Area of the grid cell (m²) and n_d the drainable porosity.

Weiler & McDonnell (2006) implemented a function for drainable porosity based on field observations, which represents the decline of n_d with depth:

$$n_d(z) = n_0 \exp\left(-\frac{z}{b}\right) \qquad \text{(Eq. 2)}$$

where n_0 is the drainable porosity at the soil surface, b is a decay coefficient, and z the depth into the soil profile where n_d should be calculated for.

Since it is assumed that the decline of drainable porosity and the decline of saturated hydraulic conductivity k_s with depth happens for similar reasons, e.g. compaction of the soil, another power law presented by Rupp & Selker (2005) was implemented:

$$k_s(z) = k_0 \exp\left(-\frac{z}{m}\right) + k_c \qquad \text{(Eq. 3)}$$

with k_0 the saturated hydraulic conductivity at the soil surface (m/s), m a decay coefficient and k_c the constant hydraulic conductivity at the deepest point of the profile, for example the soil-bedrock interface.

The saturated zone is balanced by lateral in- and outflow, the input from the unsaturated zone, the corresponding water table change, seepage to the bedrock and the in- and output form pipe flow.

Significant lateral subsurface flow happens under saturated conditions and is often triggered by a perched water table within the soil, on soil interfaces or on the soil-bedrock interface, converting the unsaturated to a saturated zone (Weiler & McDonnell 2004). So lateral subsurface flow q in the model is only allowed in the saturated zone and is calculated with the Dupuit-Forchheimer assumption (Freeze & Cherry 1979):

$$q(t) = T(t)\beta w \qquad \text{(Eq. 4)}$$

where T is the transmissivity (m^2/s), β is the water table slope and w is the width of the flow (m). Routing is then calculated with a call by call approach from Wigmosta & Lettenmaier (1999), following the local water table gradient.

Bedrock seepage S was first presented by van Meerveld & Weiler (2008):

$$S(t) = k_b(1 + w(t)) \qquad \text{(Eq. 5)}$$

with k_b the saturated hydraulic conductivity of the bedrock and w the water table height above the soil-bedrock interface. Water that leaks to the bedrock is subducted from the water balance.

The calculation of the water balance of the unsaturated zone is made by the input from precipitation and vertical drainage loss to the saturated zone. Drainage from the unsaturated zone again is controlled by a power law, depending on relative saturation, the conductivity at the water table surface and a power law exponent c (Weiler & McDonnell 2007).

In this version actual evapotranspiration from the unsaturated zone is neglected since the sprinkling experiments had a maximum duration of 12 hours.

Another important process is the lateral flow in soil pipes implemented by Weiler & McDonnell (2007).

5.2.2. Pipe flow

Pipe flow is initiated as soon as the water table of a grid cell reaches the height of an inlet to a pipe. Water flow then is proportional to the hydraulic head above a pipe and a constant that is related to hydraulic conductivity of the soil matrix, internal pipe roughness and tortuosity, hydraulic gradient, and pipe dimension (Sidle et al. 1995). Weiler (2005) complements that pipe dimension does not usually restrict pipe flow. In Hill-Vi the pipe flow q_p is then calculated according to Weiler & McDonnell (2007) by:

$$q_p(t)=k_p A^{0.5}(w(t)-z_p)^{\alpha} \qquad \text{(Eq. 6)}$$

with k_p a constant for pipe flow including hydraulic conductivity of the surrounding soil matrix, internal pipe roughness, and pipe tortuosity and hydraulic gradient, without considering pipe diameter, A the grid cell area, w the water table height, z_p the height of the pipe to the same datum and α the log linear regression between hydraulic head and pipe flow (Sidle et al. 1995), which is usually kept close to 0.4.

Pipe geometry is defined by pipe density, that is the fraction of grid cells where pipes start, and the mean and standard deviation of the height of pipes above the bedrock or whatever base for the hillslope is chosen (Weiler & McDonnell 2007).

A pipe can transmit water only to neighboring cells and are always orientated downslope. Still downslope direction is chosen randomly from all possible downslope directions. The model follows the assumption that no water is lost during the flow in the pipe. So the outflow of the pipe in the end cell is equal to the inflow in the start cell. The transported water is then added to the saturated zone of the end cell (Weiler & McDonnell 2007).

5.2.3. Root concept in the model

Following the data derived by the literature research a couple of new parameters had to be added to the model version described above.

In general these Parameters concern root geometry and are listed in Table 4.

Table 4: Parameters added to calculate root geometry

Parameter	Description
Tree density	Density of trees on the stand given in trees per hectare. Needed to generate a set of random positions of the trees on a plot.
Minimum distance	Minimum distance between two trees given in meter. Needed to resemble a more or less natural positioning due to competitive growth.
Coarse roots	Number of coarse root branches.
Depth	Depth of the location where a root grows out of the stem given in meter. Can be one value for the mean depth, if depth is distributed normally, or a range for a uniform distribution of depth.
Standard deviation of depth	Standard deviation for the depth of the root given in meter. Only needed if the depth is distributed normally.
Length	Mean length of the root branch given in meter.
Standard deviation of length	Standard deviation for the length of a root branch given in meter.
Angle	Boolean variable to determine if there is a downward angle of the root system or not.
Depth of rooted topsoil	Depth of the rooted soil given in meter. Needed to calculate the downward angle of a root, for example for European Beech.
Additional pipes	Fraction of cells where additional pipes should be placed after the root system is built.

Before generating a root geometry the positions of the trees have to be determined. One option is to create a tree map randomly by giving the tree density of the stand where the plot is located. A module then stochastically generates a table containing Cartesian coordinates of the tree's position. Giving a minimum distance between the trees guarantees that in the first place two trees do not end up in the same grid cell and in the second place the stand properties approximately resemble natural competitive growth, even if not on a level as sophisticated stand models can do. From this table a map is created which can also be exported and restored for later model runs.

The model also offers the option to read-in a root map from a table of Cartesian coordinates. This is actually the better option for sprinkling experiments because the system then is reduced by one degree of freedom and random root geometries could be compared more easily.

A tree's position defines the starting point for all its coarse roots. In the next step the number of coarse roots for each tree is read-in.

The direction a root is growing in cannot be determined by the modeler. It is chosen randomly for each root from all possible directions.

Then a starting depth for each root is determined. The model has the ability to deal with a mean value of root depth and a standard deviation to generate a single depth value, like in the original model version. Due to the lack of statistically reliable information in literature this option was not used for the current study. Instead, a range for root depth was given and treated as uniformly distributed. The depth for each root was then selected from this range.

Root length is given by a mean value of root length and its standard deviation. Assuming that the range of lateral ramification of a root does not exceed the size of a grid cell and the fact that literature just gives reliable information for the length of the main root branches, each root branch is lumped to one.

A couple of tree species under certain conditions develop their root system with a downward angle. European Beech for instance does that on soils with a structure where roots are easy to propagate. There is no general data for root angle for European Beech. But combining the data for root length and the knowledge that the angled coarse root ends on the bottom of the rooted topsoil, a downward angle could be calculated from these two parameters.

The direction of the root and its length can be used as azimuth and polar axis in a polar coordinate system. By a simple transformation to Cartesian coordinates via the trigonometric functions the roots can be stepwise routed through the grid. If there is a downward angle calculated, the routing of roots gets a downward component, which is calculated via the trigonometric functions analogously to the procedure described above. With this downward component the depth of the root for each step is manipulated, whereas it remains the same relative to the soil surface for a non-angled root system.

The stepwise routing of the root's path leads to a parting of the root and the potential pipe respectively. This implicates that each root part allows water flow just from one cell to a cell in its vicinity, adding the transmitted water to the saturated zone of the target cell. That makes flow along a root part conceptually and mathematically exactly the same like in a soil pipe in the original model. It is assumed that this concept resembles the water flow along a root best, since each tree species used, especially Norway Spruce, has sinker roots or comparable root structures heading to the water table surface. Also pipe flow can be initiated on any point along a root, if a transient water table reaches it.

Pipe flow on roots can just happen from the higher to the lower end of the root part, both relative to the same datum. For a root system without a downward angle this means that flow can happen from upslope in direction to the tree and from the tree in direction to the downslope roots. In case of an angled root system this can result in flow of water in upslope direction, in case the transient water table is high enough to generate a sufficient hydraulic gradient.

Creating a root geometry for a couple of trees with the procedure described above, it is almost certain that, given a natural tree density and number of coarse roots, some roots cross each other's path. Another routine implemented in the new model concept makes sure that all root parts in a cell are sorted according to their height. This guarantees that pipe flow first happens along the lowest root part. The next higher part only reacts if there is still enough water left in the current grid cell to let the water table rise above the location of the root part.

Both Jost (2004) and Nordmann et al. (2009) mention a loss of water in the mass balances calculated after the sprinkling experiments. One reason according to the authors is bedrock seepage, which is described above. Another important factor mentioned is the loss caused by lateral subsurface flow out of the plot, both by matrix and preferential flow. Lateral matrix flow out of the plot is assumed to be neglectable in a timescale of less than 10 hours. But to meet the loss of water by preferential flow, roots growing out of the plots are allowed to transport water out. This water is subducted from the balance, analogously to bedrock seepage, and is lost to the domain.

After this it is optional to define a fraction of cells still without a root to get a random pipe. These pipes are then built similar to the old concept.

The model is just able to deal with one tree species per plot.

5.3. Modeling

The first approach to analyze the new model structure was to calibrate the model to the sprinkling experiments described above.

For each of the plots 2500 Monte-Carlo runs were carried out for all six plots and efficiencies after Nash & Sutcliffe (1970) (n_{eff}) were calculated to evaluate the agreement with the measured runoff. Efficiencies and parameter values are then plotted against each other in dot plots.

Table 5 shows the parameters which were used for the calibration of the plots.

Table 5: Parameters for calibration

Parameter	Description
k_p	Multiplicative constant for determining the inflow into the pipe
n	Total porosity (-)
n_d	Drainable Porosity (-)
b	Decay coefficient for drainable porosity
k_0	Saturated hydraulic conductivity at soil surface (m/h)
m	Decay coefficient for saturated hydraulic conductivity
k_b	Hydraulic conductivity of bedrock for bedrock seepage (m/h)
θ_0	Initial relative water content in unsaturated zone (-)

During these first runs the model showed some deficits despite some very high efficiencies. For example half of the modeled runoff was surface runoff. The calibrations were made anyway to test the sensitivity of some parameters and to see if some parameters could be ignored in the oncoming calibrations. The results and the possible errors are presented and discussed below.

As a first modification random pipes were added for each cell without a root to assure sufficient drainage. Another 2500 Monte-Carlo runs were then carried out to calibrate the plots B1, B2, S1 and S2. For this the parameters from Table 5 were used as well. Again dot plots were generated.

Then a validation of these parameters with the plots B3 and S3, which are, besides size, of the same features as the other plots, was tried. The plots were then calibrated as well to compare them to the parameters formerly used as input.

Afterwards the two plots with the highest efficiencies, plot B2 and S2, were taken to vary the root parameters and to test their sensitivities. The parameters varied were:

- Coarse roots
- Length
- Standard deviation of length
- Additional pipes

from Table 4.

Finally the ranges of the parameters 'Coarse roots' and 'Length' were divided into classes and plotted in dot plots to test their dependencies on each other.

6. Results

In the following the results from the proceeding described in chapter 5.3. is presented.

Introductorily a couple of facts from the chapters above should be remembered, when results are examined. B1, B2 and S1 are experiments from the Kreisbach catchment, while B3, S2 and S3 are from the Frankenwald. That includes on the one hand that each plot of a group has approximately similar soil properties and size, and, on the other hand, received the same treatment, both in regards to the experiment's design and under the consideration that they were conducted by the same researchers. But the two groups differ especially in plot size.

Another thing to remember introductorily is that B1 and B2 are actually the same plot, but split into two modelings due to the sprinkling issues mentioned above. So special caution is recommended during the view on the results of these two experiments.

6.1. Calibration without additional pipes

The parameter combinations that achieved the best agreements to runoff data according to n_{eff} are given in Table 6. The parameter ranges used for calibration are the same as given in the figures of chapter 6.2.

It is to be mentioned here that these results were just presented to show that although a big part of the runoff modeled was generated by overland flow, efficiencies are quite high. In general all plots reached efficiencies above 0.7. The highest agreement is reached by the spruce-plot S2, closely followed by the beech-plot B3. Both are plots from Frankenwald.

B1 and B2 showed comparable results for the pipe constant k_p and the total porosity n. Also the relative initial water content is quite similar for both modelings. The other parameters differ significantly.

B3 and S2, which are located in direct vicinity to each other on the same stand, also reached comparable results for the pipe constant, the total porosity and the initial water content.

The values for both decay coefficients, m and b, vary over the whole range. The values for relative initial moisture content θ_0 are all around 40 percent.

Table 6: Calibration without additional pipes

Parameter	B1	B2	B3	S1	S2	S3
n_{eff}	0.865	0.742	0.871	0.807	0.888	0.777
k_p	253.81	256.78	176.51	153.98	150.17	29.47
n	0.470	0.461	0.538	0.476	0.546	0.497
n_d	0.0367	0.0042	0.0151	0.1164	0.0413	0.0996
b	1.61	2.83	1.41	2.28	3.60	2.69
k_0	0.0035	0.0542	0.0310	0.0150	0.0218	0.1373
m	2.13	1.57	2.90	1.27	1.44	2.81
k_b	0.00006	0.00074	0.00100	0.00100	-	0.00016
θ_0	0.400	0.377	0.411	0.421	0.437	0.375

Figure 11 shows the root geometry of a slope without additional pipes in the model and the effects of the root geometry on overland flow.

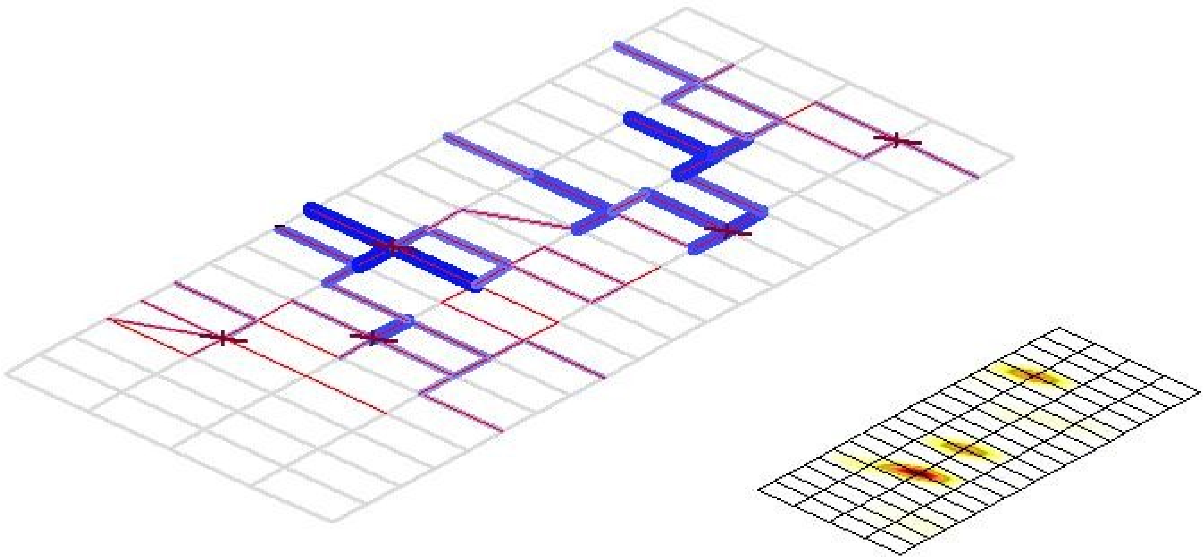

Figure 11: View of the root geometry of a spruce in the model with pipe flow (large) and overland flow (small).
The crosses mark the positions of the trees and the red lines the roots. Blue lines mark the pipe flow along roots. The thicker the line is, the more flow happens. The yellow and reddish areas show where overland flow occurs, with yellow few and red much flow.

The larger image shows the grid, which represents the slope, with the positions of the trees and the simulated root network. The image is a bit compressed though. Grid cells are actually squares with 1 meter length. The downslope trench would be at the left end of the grid.

In this example it is remarkable that no root reaches the trench.

Upslope one can see a dead-end root, where a lot of pipe flow occurs. At the same position in the smaller picture occurs overland flow.

Also at the positions where upslope roots meet a tree or some roots converge overland flow can be seen.

Roots which end at the border of the plot and have pipe flow, but do not generate overland flow, spill the water out of the plot. The visualization of this was deactivated for a better view.

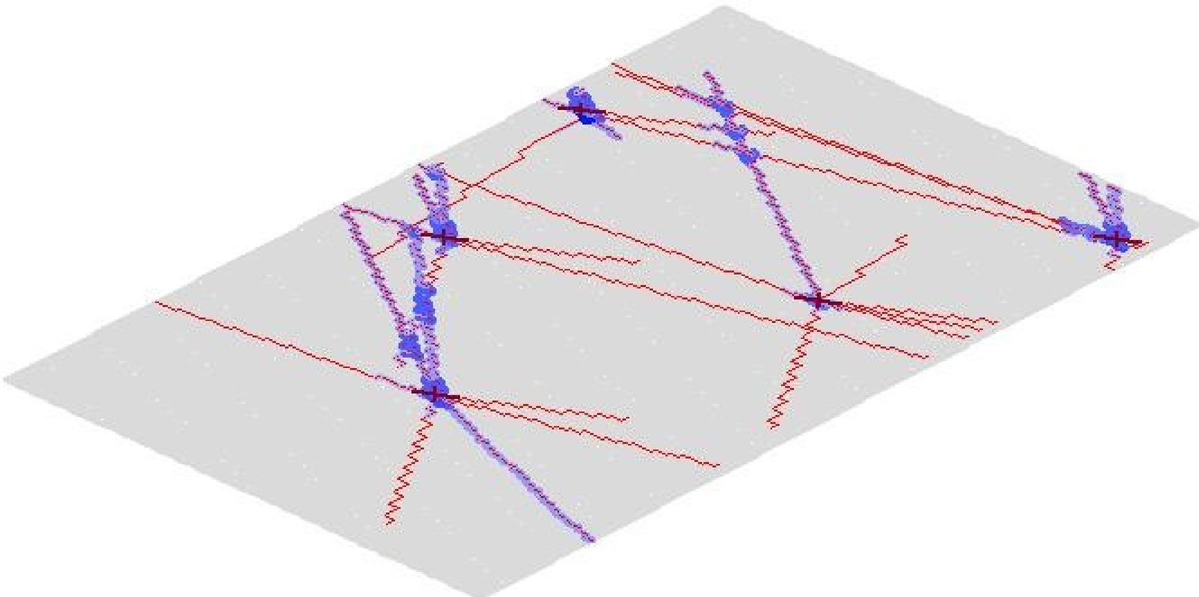

Figure 12: Visualization of a Spruce-plot with a 10 cm grid.

Figure 12 shows exemplaryily how the root geometry would look like, if a 10 cm grid was used. Modeling with a grid with less than 1 meter size resulted in extraordinarily long simulation times, so this option was not explicitly tested. Still this gives an impression of how stochastic artificial root systems develop.

It also shows, as mentioned above, how intensively water can accumulate where roots cross or converge at trees.

6.2. Calibration with additional pipes

After the physically rather wrong results from the calibration without additional pipes, another calibration with additional pipes in each grid cell without a root part was made.

The summed up results from the calibration of B1, B2, S1 and S2 are presented in Table 7.

Table 7: Calibration with additional pipes of plot B1, B2, S1 and S2

Parameter	B1	B2	S1	S2
n_{eff}	0.825	0.864	0.879	0.938
k_p	58.10	162.26	276.17	38.18
n	0.524	0.473	0.487	0.490
n_d	0.0177	0.1757	0.0793	0.0831
b	2.71	3.38	1.32	3.03
k_0	0.0102	0.0306	0.0061	0.0272
m	1.31	1.05	2.02	1.02
k_b	0.00031	0.00032	0.00091	0.00095
θ_0	0.408	0.423	0.426	0.392

The results of the 2500 Monte-Carlo runs to vary parameters are given as dot plots. The ranges in which the parameters were varied are equal to the ranges labeled to the abscissa. The black points represent model runs with the actual parameter value against the efficiency. The values from the runs with the most efficient parameter sets are indicated as gray diamonds.

In the dot plots only values are considered that reached an efficiency higher than 0. The number of runs where this applies varies between plots, but is especially low for the spruce-plots.

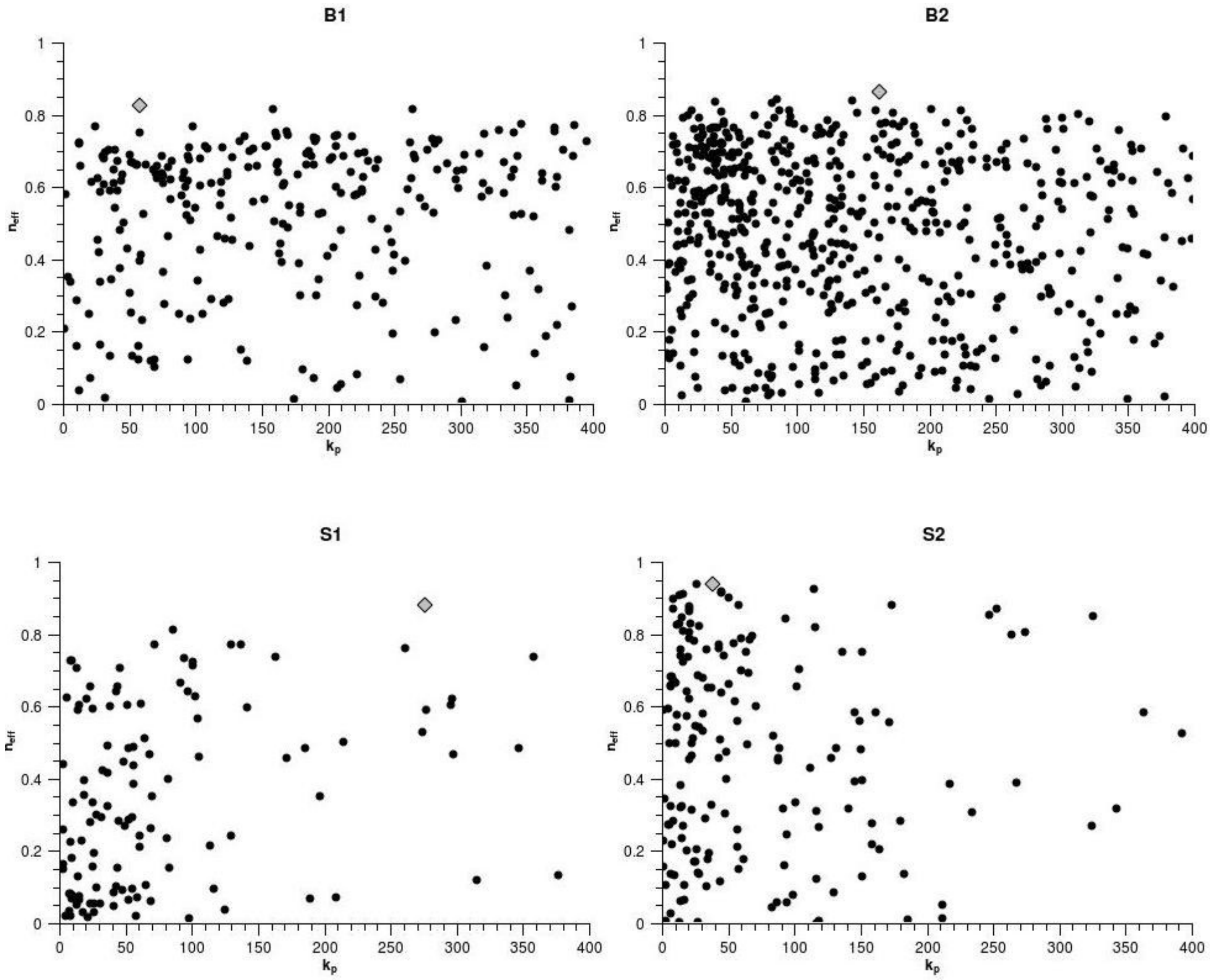

Figure 13: Pipe constant against efficiency. Best values are represented by diamonds.

The results from the variation of the pipe constant k_p are given in Figure 13.

There is no distinct peak of efficiency in any plot. Maximal values rather spread over the whole range. One remarkable feature is the exposed best value in S1, what is in opposite to the other remarkable feature, which is the higher density of dots in the lower half of the range. So most of the runs, which reached efficiencies above 0, had values about below 150.

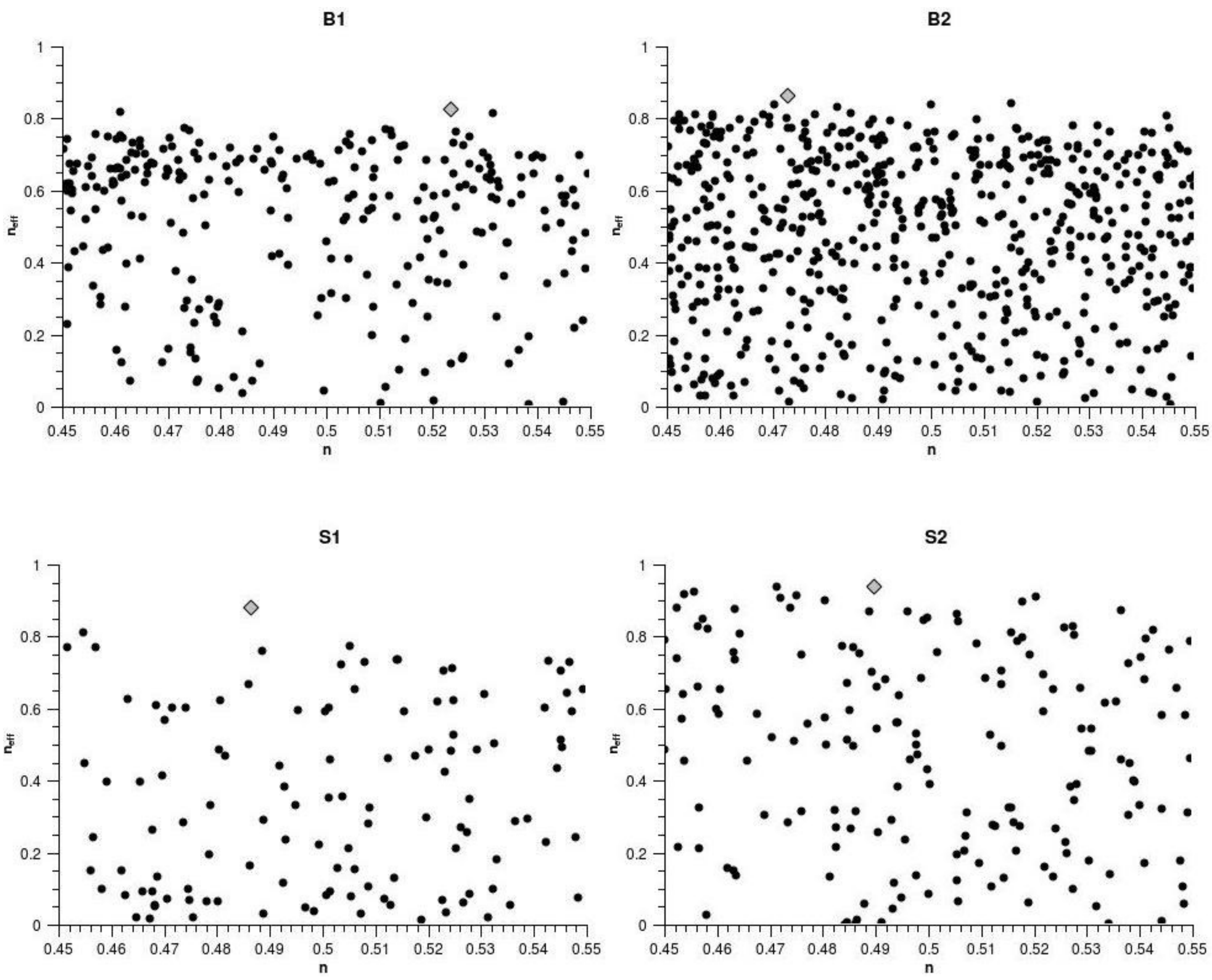

Figure 14: Total porosity against efficiency. Best values are represented by diamonds.

Same is true for the dot plots of the total porosity *n* (Figure 14). The variance is quite homogeneous. B1 tends a little to a higher value, while B2, S1 and S2 stay below 0.49.

The situation differs totally for drainable porosity n_d (Figure 15). Especially B1 and S1 show a clear trend towards low values, while S1 almost shows a kind of peak around its optimal value. S2 also has a tendency to values below 0.2, since there is a gap between this area and higher values. Still there are some high efficiencies at around 0.25.

B2, which should actually be close to B1, has more homogeneous values and a maximum above the others. Still there is a slightly higher density of dots between 0 and 0.1.

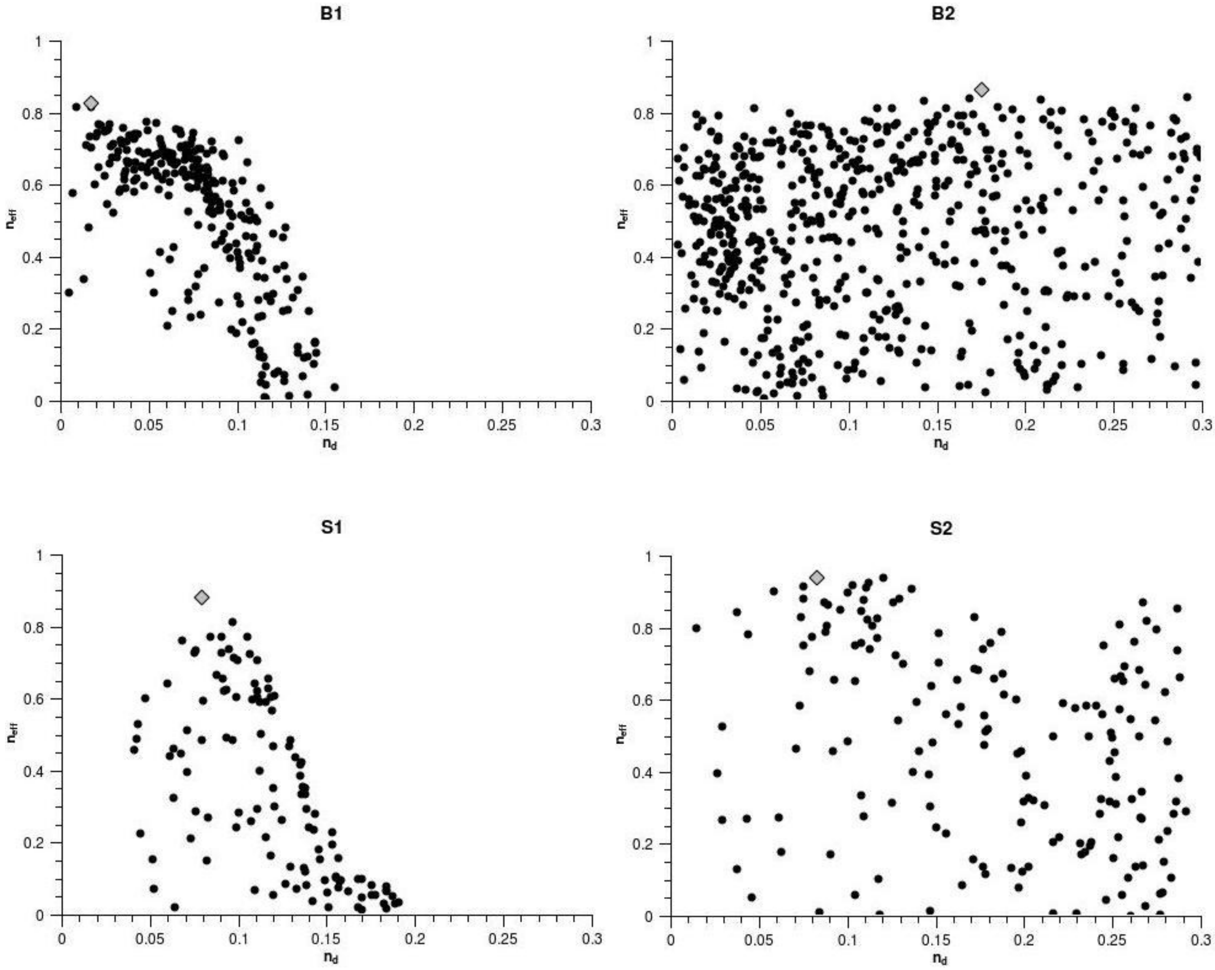

Figure 15: Drainable porosity against efficiency. Best values are represented by diamonds.

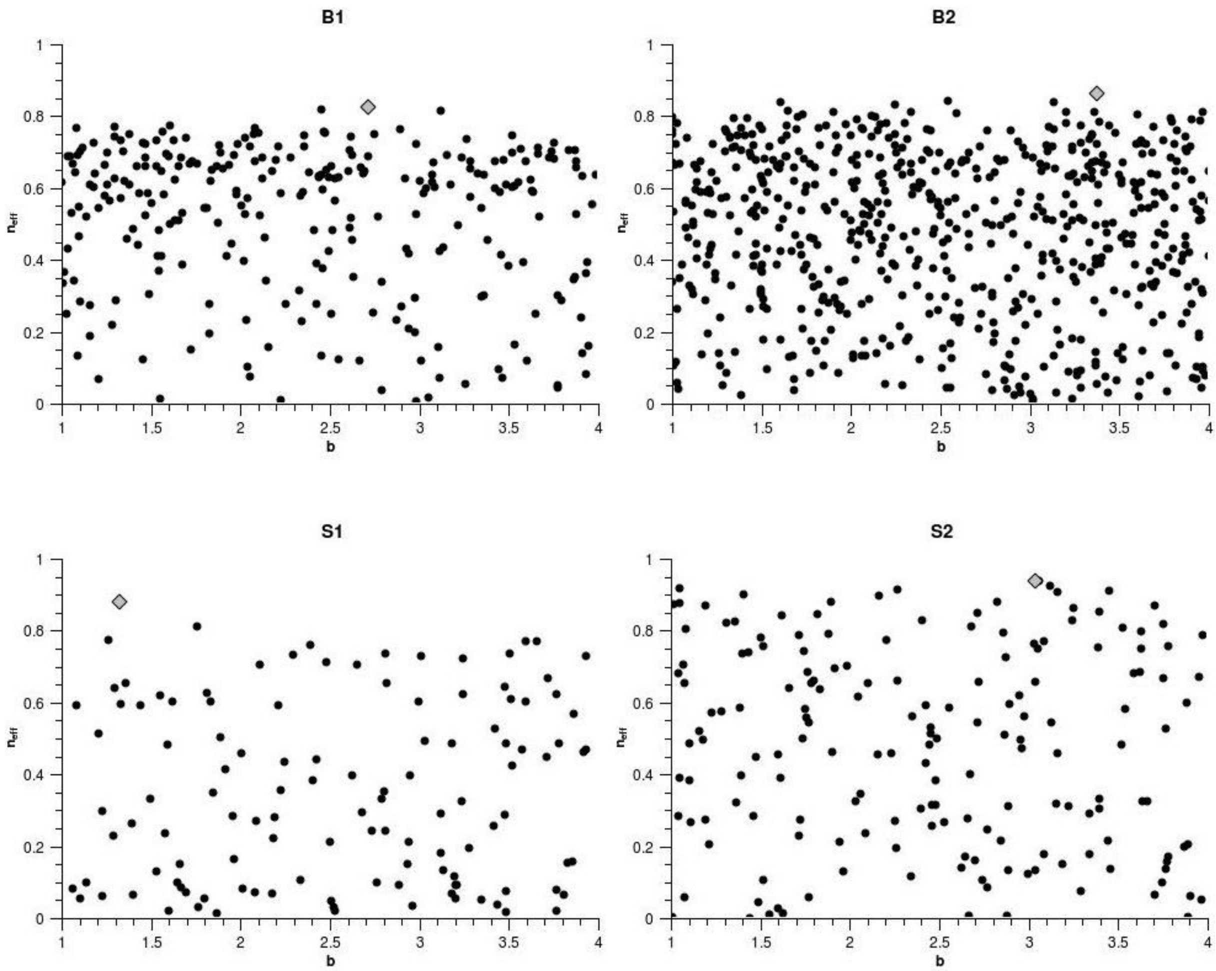

Figure 16: Decay coefficient b against efficiency. Best values are represented by diamonds.

The decay coefficients b (Figure 16) and m (Figure 18) both show low sensitivities to variation. The values for b in B1, B2 and S2 are approximately homogeneous with a tendency to have a maximum between 2.5 and 3.5.

Same applies for m, but with a tendency to values around 1.

For both parameters the situation in S1 is different. Both dot plots show behavior that differs clearly from the others. That results in a maximum for b around 1 and for m around 2.

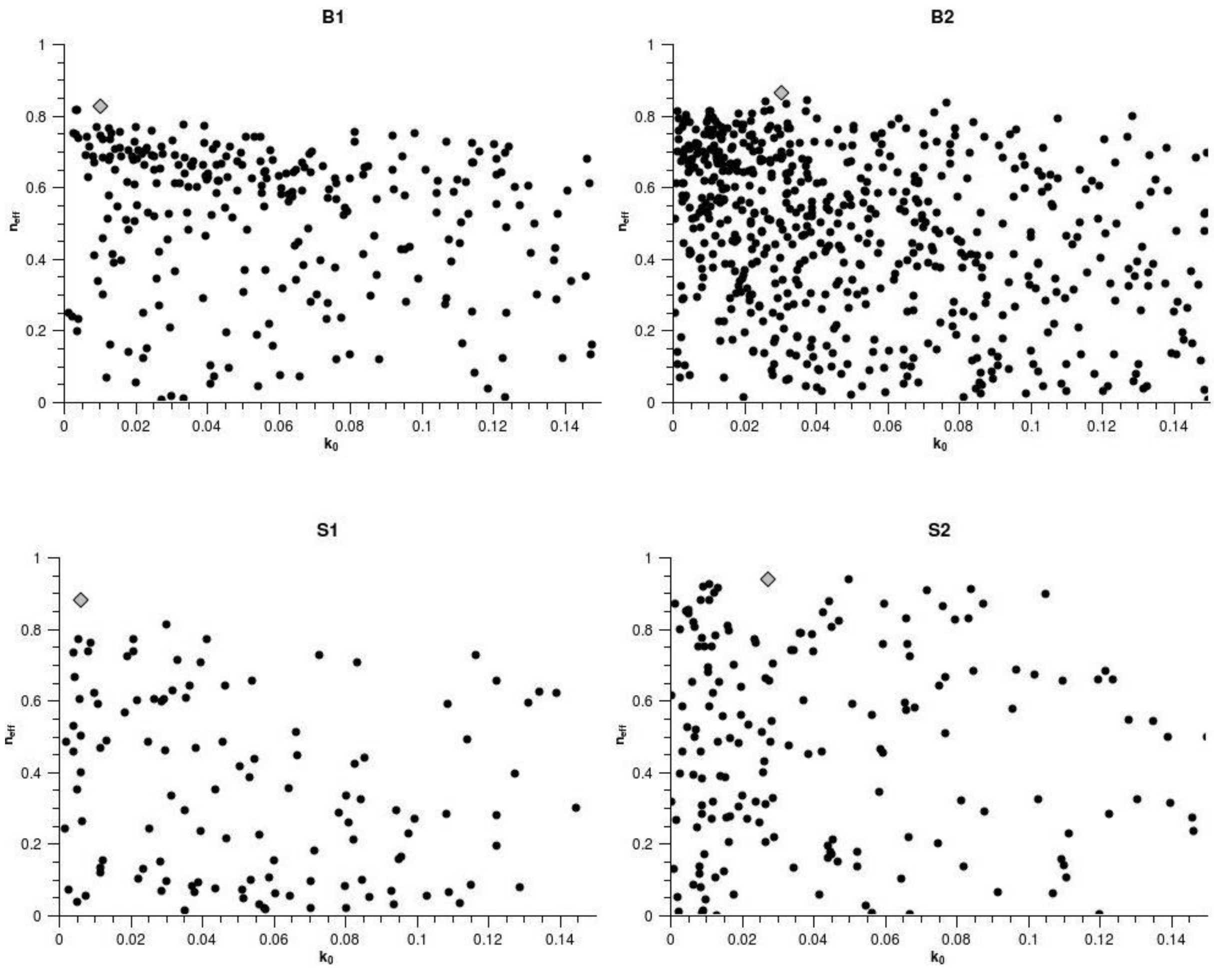

Figure 17: Saturated hydraulic conductivity at soil surface against efficiency. Best values are represented by diamonds.

Saturated hydraulic conductivity at soil surface, k_0, is shown in Figure 17. It appears that this value is the only one with clear tendencies in all modelings. The best values are all settled between 0.006 and 0.03, and show a clear overall tendency towards low values.

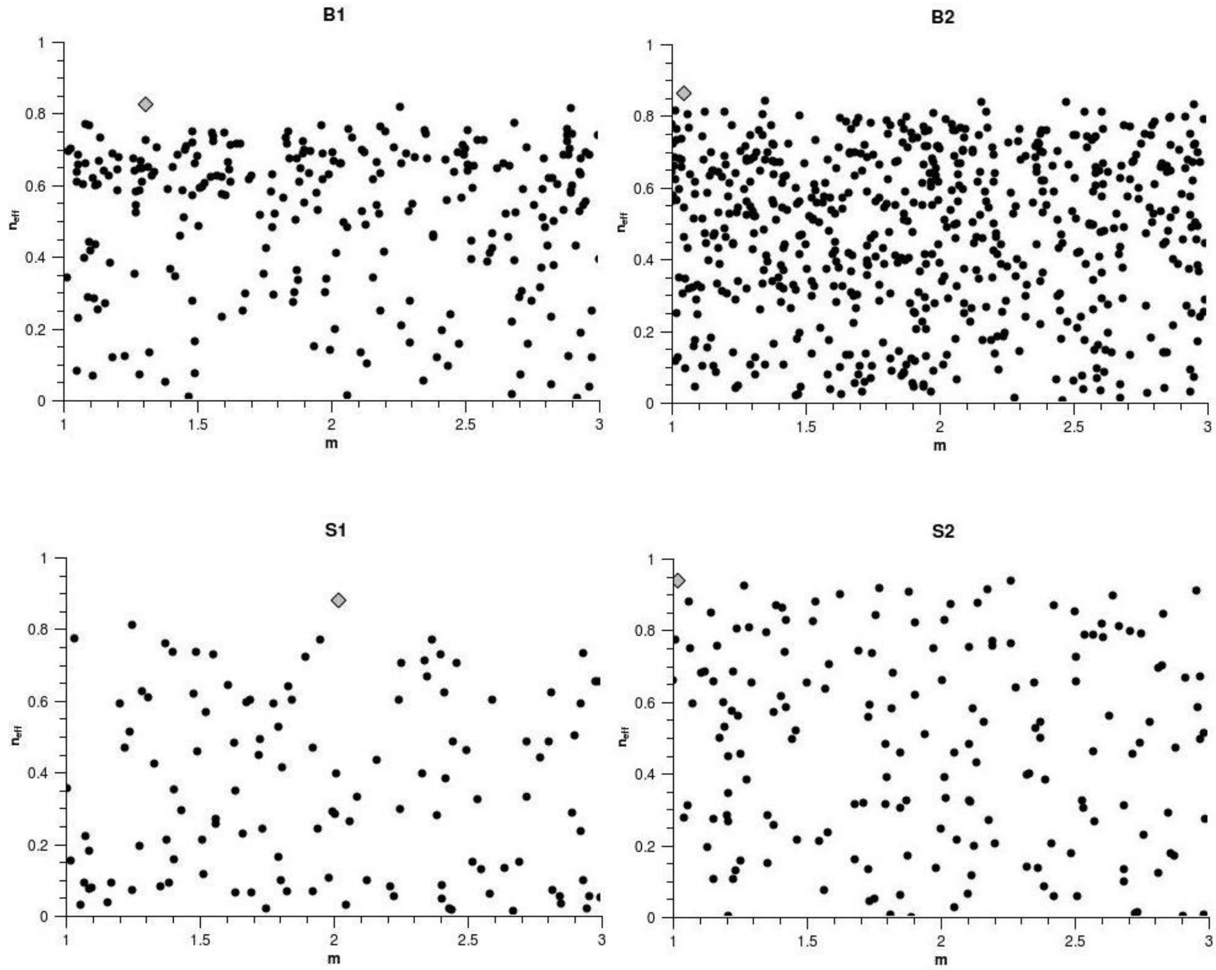

Figure 18: Decay coefficient m against efficiency. Best values are represented by diamonds.

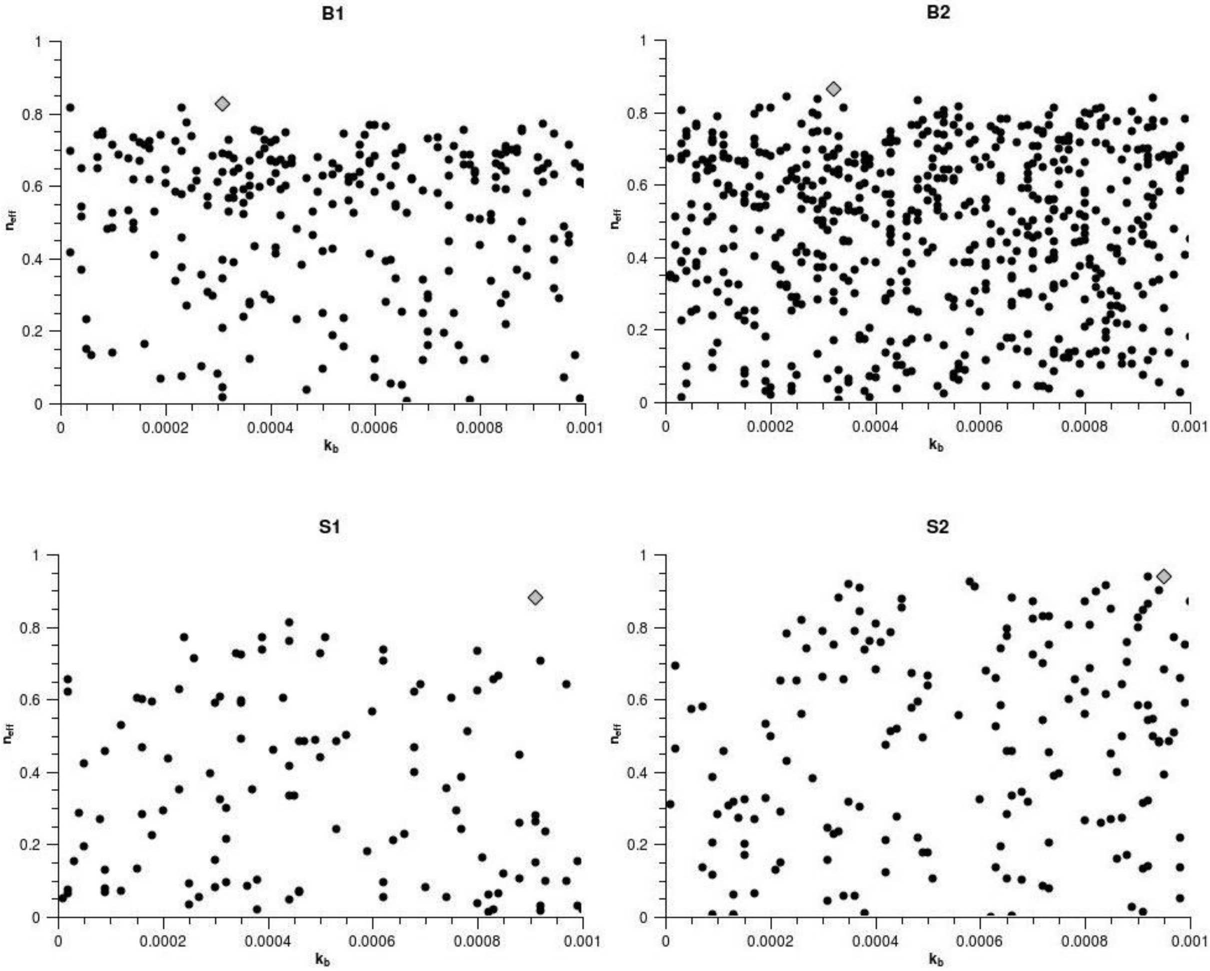

Figure 19: Saturated hydraulic conductivity of bedrock against efficiency. Best values are represented by diamonds.

The values for saturated hydraulic conductivity of bedrock, k_b, are rather grouped by tree species. S1 and S2 both show the tendency to high values, while the maximum is located at the rim of the range. B1 and B2 both tend to best values around 0.0003 but do not show the clear tendency as the spruce-plots do.

The values for the initial relative water content θ_0 for B1, B2 and S1 all range around 0.41 to 0.42. Only S2 shows a significantly lower value.

B2 is a little higher than B1, which is connected to the fact, that there was only a short break between the two sprinkling experiments on the same plot. Because of this only for B2 the initial water table was calibrated additionally. This parameter seems to maximize around 0.4.

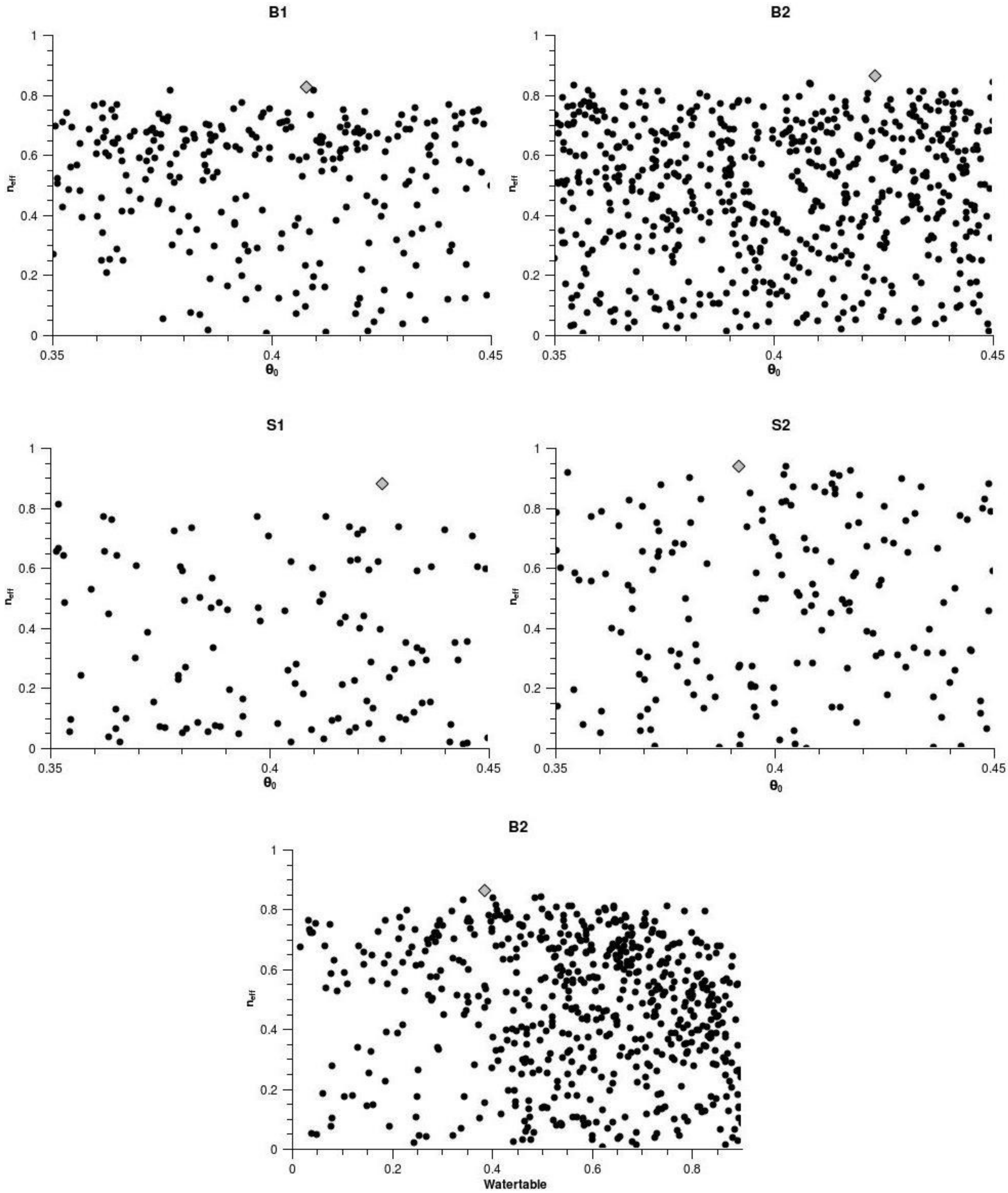

Figure 20: Initial relative water content (top) and the initial watertable of plot B2 (bottom) against efficiency. Best values are represented by diamonds.

6.3. Validation

The knowledge gathered from the calibrations presented above was used to verify the model concept in 100 runs with varying pipe geometry. The results from this validation are presented separately for each input parameter set in Figure 21. The gray lines are the best 20 model runs. Their efficiency ranges are given in Table 8.

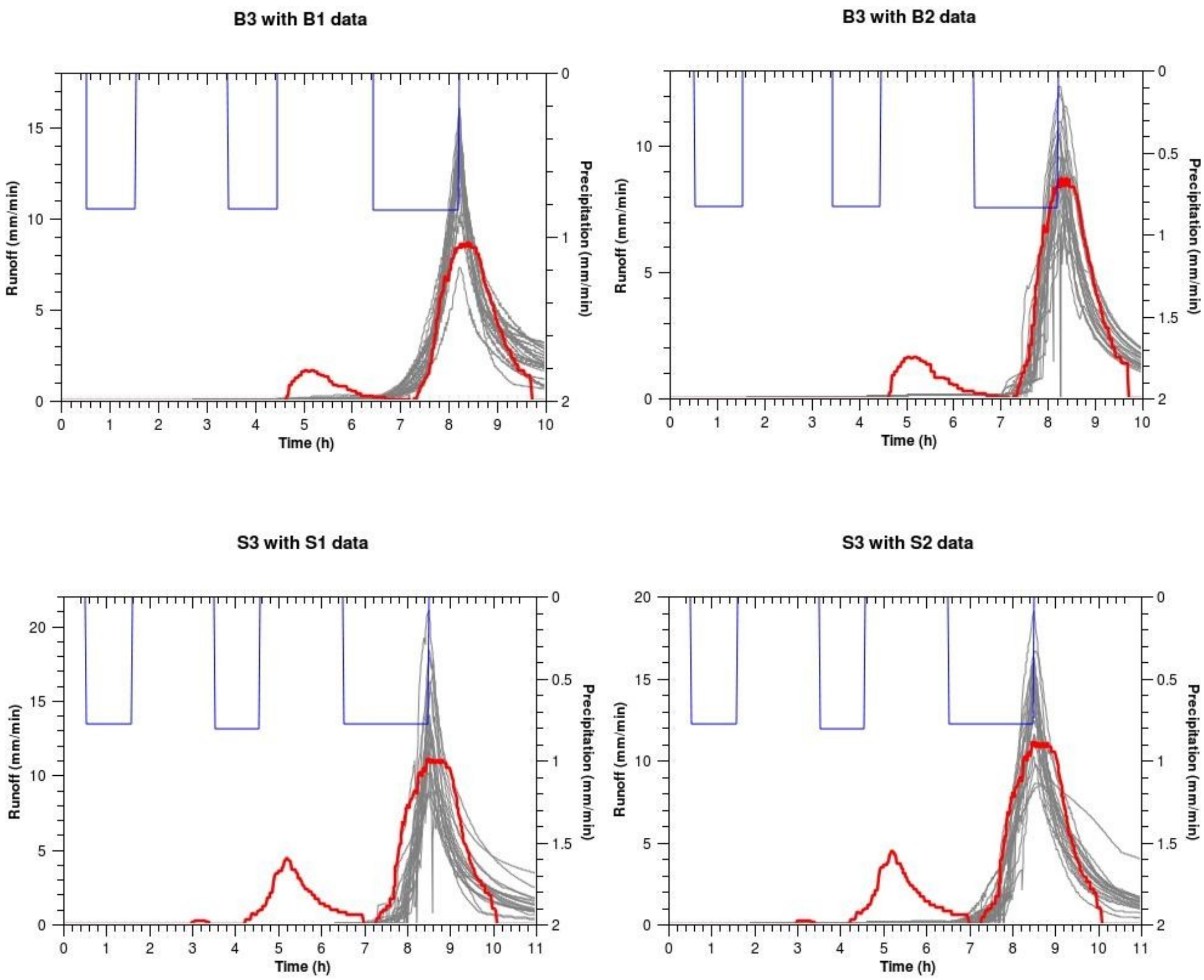

Figure 21: Validation with plot B3 and S3
Red line is the measured hydrograph, gray lines are the hydrographs of the 20 best model runs, blue rectangles are precipitation input from sprinkling.

Similar to the measured runoff the model does not noticeably react to the first input from precipitation.

The model does also not react to the second input signal from precipitation. Only the two beech-plots rise slightly, but not significantly compared to measurement.

The reaction to the third input signal is almost on time with the measurement. In exchange most model runs overestimate the peak by nearly the factor 2.

Table 8: Efficiency range from validations

	Low	High
B3 with B1	0.63763	0.84263
B3 with B2	0.75327	0.90001
S3 with S1	0.37142	0.59459
S3 with S2	0.53787	0.7595

The efficiencies of the beech-plots in general tend to higher values. Also the ranges, where the 20 best efficiencies lie, are a little narrower. In fact, the beech-runs did not produce a single efficiency below 0, which does not apply to the spruce-runs.

6.4. Calibration of plot B3 and S3

To complete the calibrations with additional pipes, the validated plots were calibrated to.

Table 9: Calibration with additional pipes plot B3 and S3

Parameter	B3	S3
n_{eff}	0.775	0.819
k_p	287.25	32.56
n	0.529	0.481
n_d	0.0123	0.2514
b	2.43	3.57
k_0	0.0018	0.0778
m	2.97	2.75
k_b	0.00043	0.00095
θ_0	0.361	0.448

Table 9 shows the best parameter sets and efficiencies for the calibration. Analogous to the calibrations in chapter 6.2. dot plots were generated. Again the spruce-plot produced more parameter sets with efficiencies above 0.

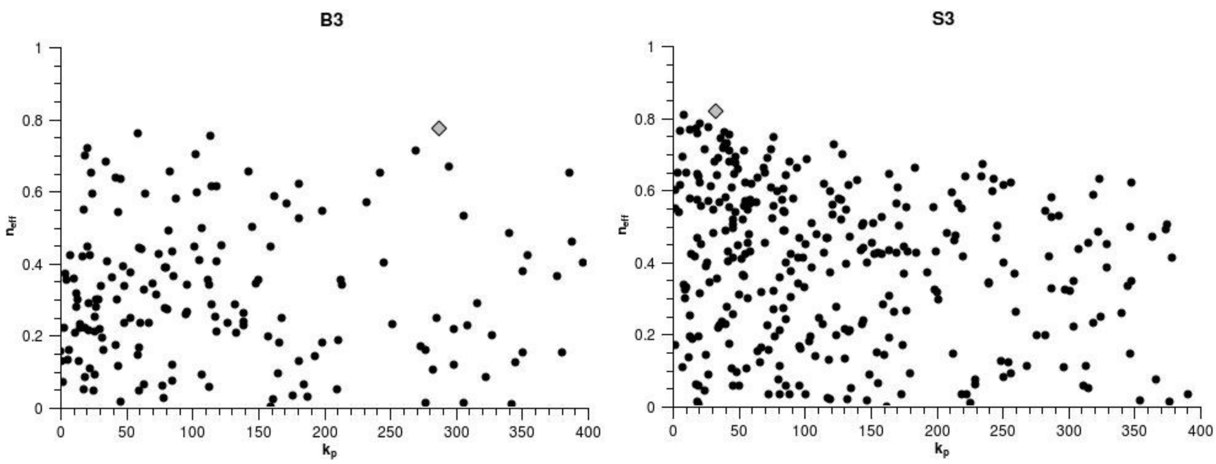

Figure 22: Pipe constant against efficiency. Best values are represented by diamonds.

Similar to the behavior in the previous calibrations the pipe constant k_p (Figure 22) shows a higher density of dots in the lower half of the range. Of all calibrations, S3 is the only plot showing a significant tendency to low values for the pipe constant.

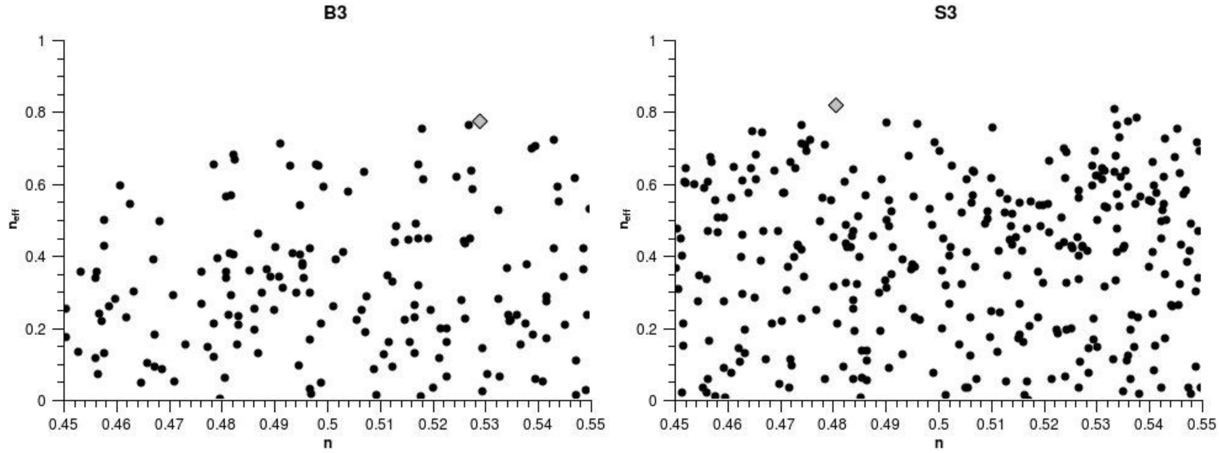

Figure 23: Total porosity against efficiency. Best values are represented by diamonds.

For the total porosity n (Figure 23) the situation stays comparable to the calibrations above. The variance is quite homogeneous with B3 having a slight tendency towards higher values. Like B1, B3 has its best value at around 0.53. Similar to the other spruce-plots, the best value for S3 is below 0.49.

Again, drainable porosity n_d (Figure 24) has distinguishable peaks. B3 behaves like the plots above, with best values in the lower part of the range, having a maximum at around 0.01.

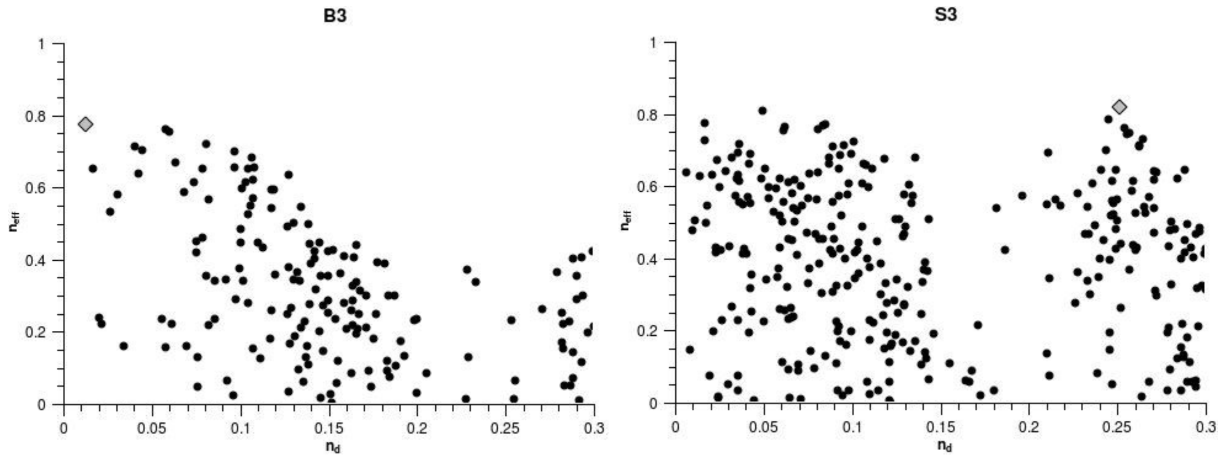

Figure 24: Drainable porosity against efficiency. Best values are represented by diamonds.

S3 also shows a peak at low values, but has a second peak at around 0.26. This is a remarkable feature and Table 9 first gives the impression of an outlier. But around this value some others are grouped. Nevertheless there are a lot of runs with efficiencies close to the optimal values in the lower half of the range.

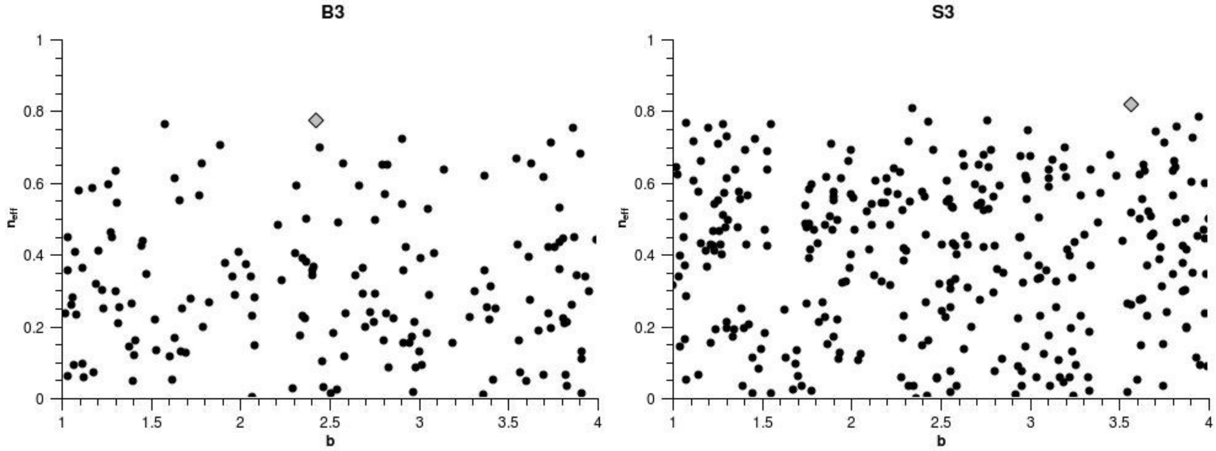

Figure 25: Decay coefficient b against efficiency. Best values are represented by diamonds.

In this calibration the decay coefficient *b* (Figure 25) behaves for both plots similar to the calibrations above. The variance is homogeneous and best values are around 2.5 and higher.

The decay coefficient *m* (Figure 27), instead, tends to the same behavior as S1, which was previously considered as outlier. Values are quite high and tend to the edge of the range. Still the variance is rather homogeneous.

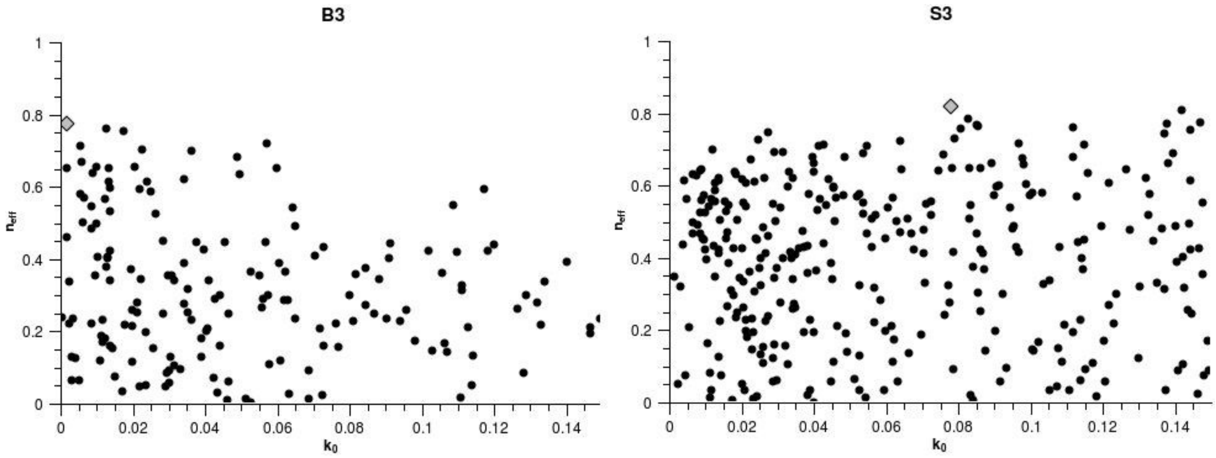

Figure 26: Saturated hydraulic conductivity at soil surface against efficiency. Best values are represented by diamonds.

The saturated hydraulic conductivity at soil surface k_0 (Figure 26) shows for B3 the same results as above. Values tend to be low and the maximum is at the very end of the range. The situation seems upside-down for S3. The tendency rather goes towards higher values and the best value is the highest in all calibrations.

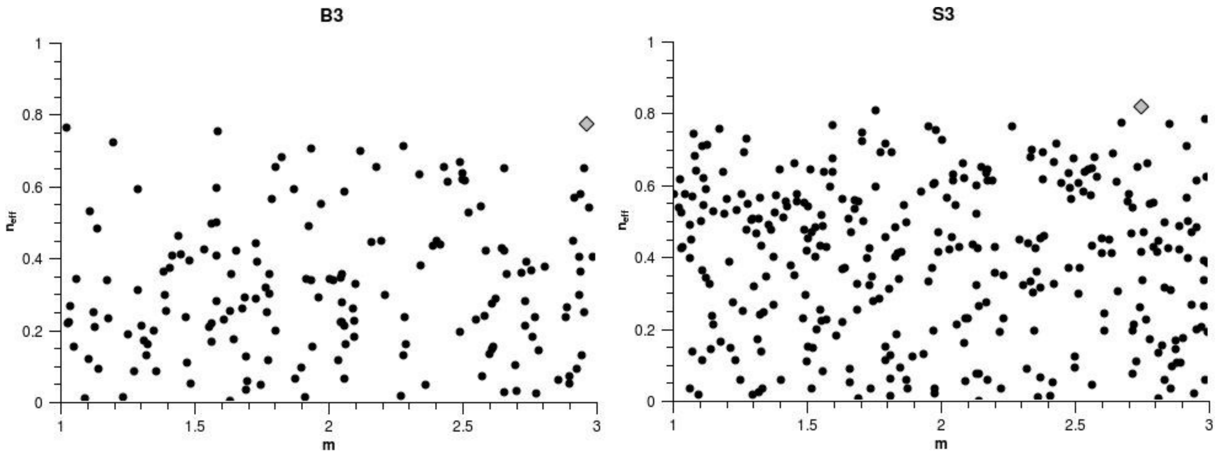

Figure 27: Decay coefficient m against efficiency. Best values are represented by diamonds.

The saturated hydraulic conductivity of bedrock k_b (Figure 28) behaves all in all similar to the calibrations above. Beech has its best value around the average of the range, while the best value for spruce is on the upper end, with a general tendency towards high values.

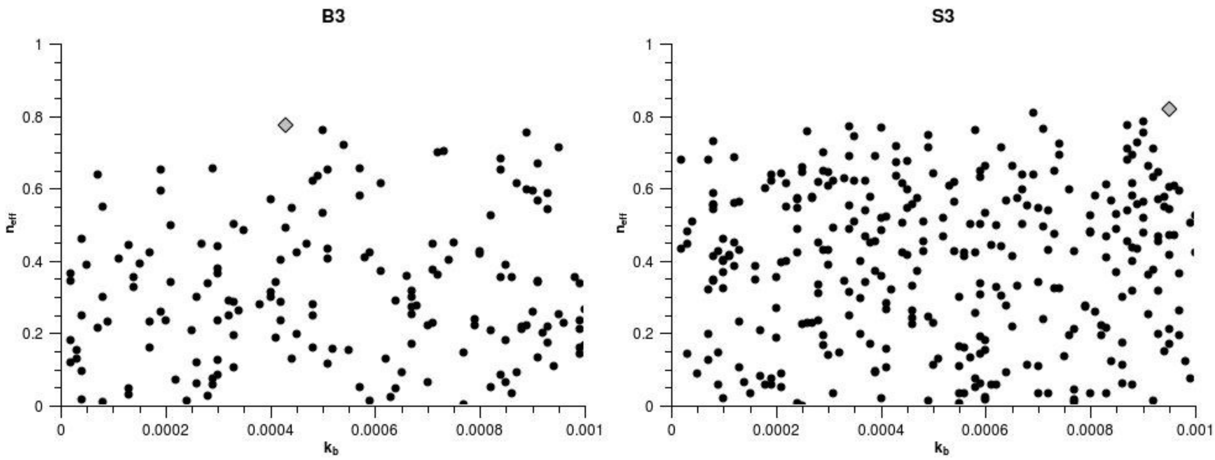

Figure 28: Saturated hydraulic conductivity of bedrock against efficiency. Best values are represented by diamonds.

The values for the initial relative water content θ_0 (Figure 29) shows just slight tendencies, but do not behave like the first calibrations. Remarkable though is, that the best values stand at the opposite end of the ranges and differ at least by 0.02 to the values from the other plots.

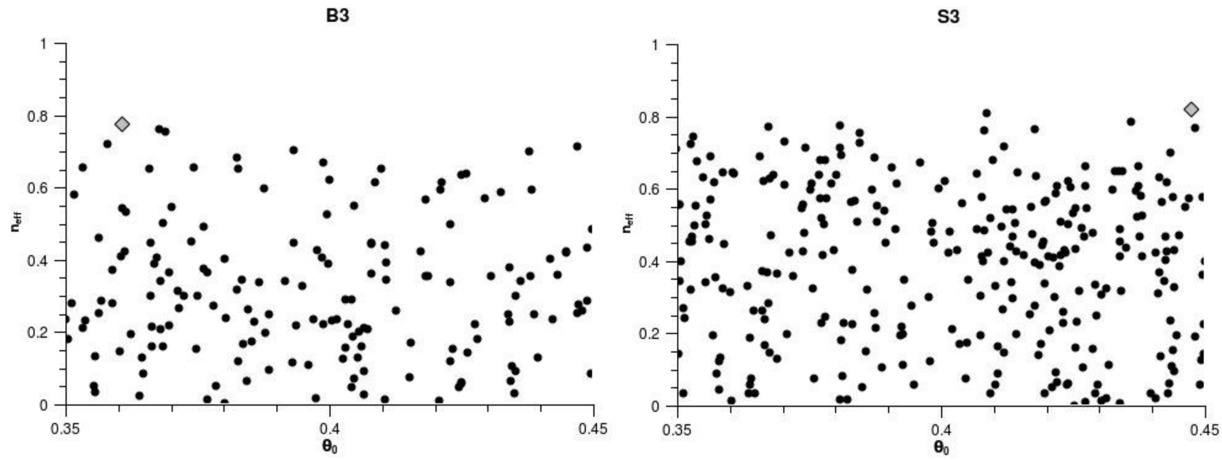

Figure 29: Initial relative water content against efficiency. Best values are represented by diamonds.

6.5. Variation of root parameters

Similar to the calibrations described above, the root parameters from the 2500 Monte-Carlo runs to calibrate the model are plotted in dot plots. The parameter sets with the highest efficiencies are marked by yellow diamonds. This time two parameters, coarse root number and root length, are additionally divided in classes to track their dependencies on other parameters.

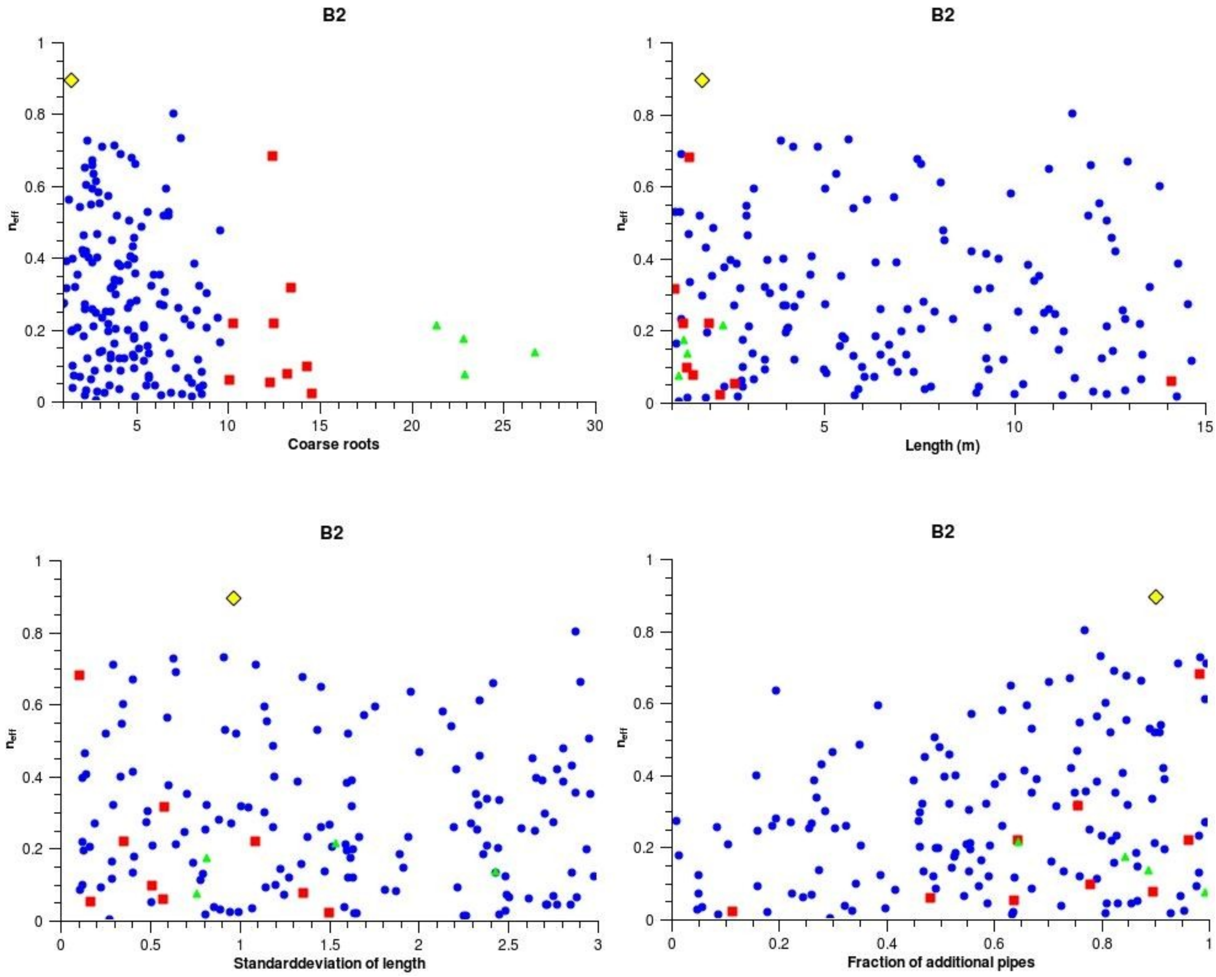

Figure 30: Variation of root parameters for plot B2 with coarse root number classified. Blue is coarse root number from 1 to 10, red from 11 to 20 and green from 21 to 30. Best values are represented by yellow diamonds.

Figure 30 and Figure 31 show the results from calibration for the beech-plot B2, Figure 32 and Figure 33 for the spruce-plot S2.

First remarkable difference between the two plots is, that this time, the beech-plot has fewer parameter sets above an efficiency of 0 than the spruce-plot. But still it reaches efficiencies up to 0.9 (compare Table 9).

The number of coarse roots for B2 shows a clear tendency towards low values, as the best value suggests. Almost all of the dots are in the area below 10. Just a few, with all in all low efficiencies, are with higher values.

Root length and its standard deviation both do not show this tendencies, but have both their best value clearly around 1.

The parameter for the fraction of additional pipes again has a clear tendency towards high values. With a best value around 0.9 the most of the higher efficiencies lie in the upper half as well.

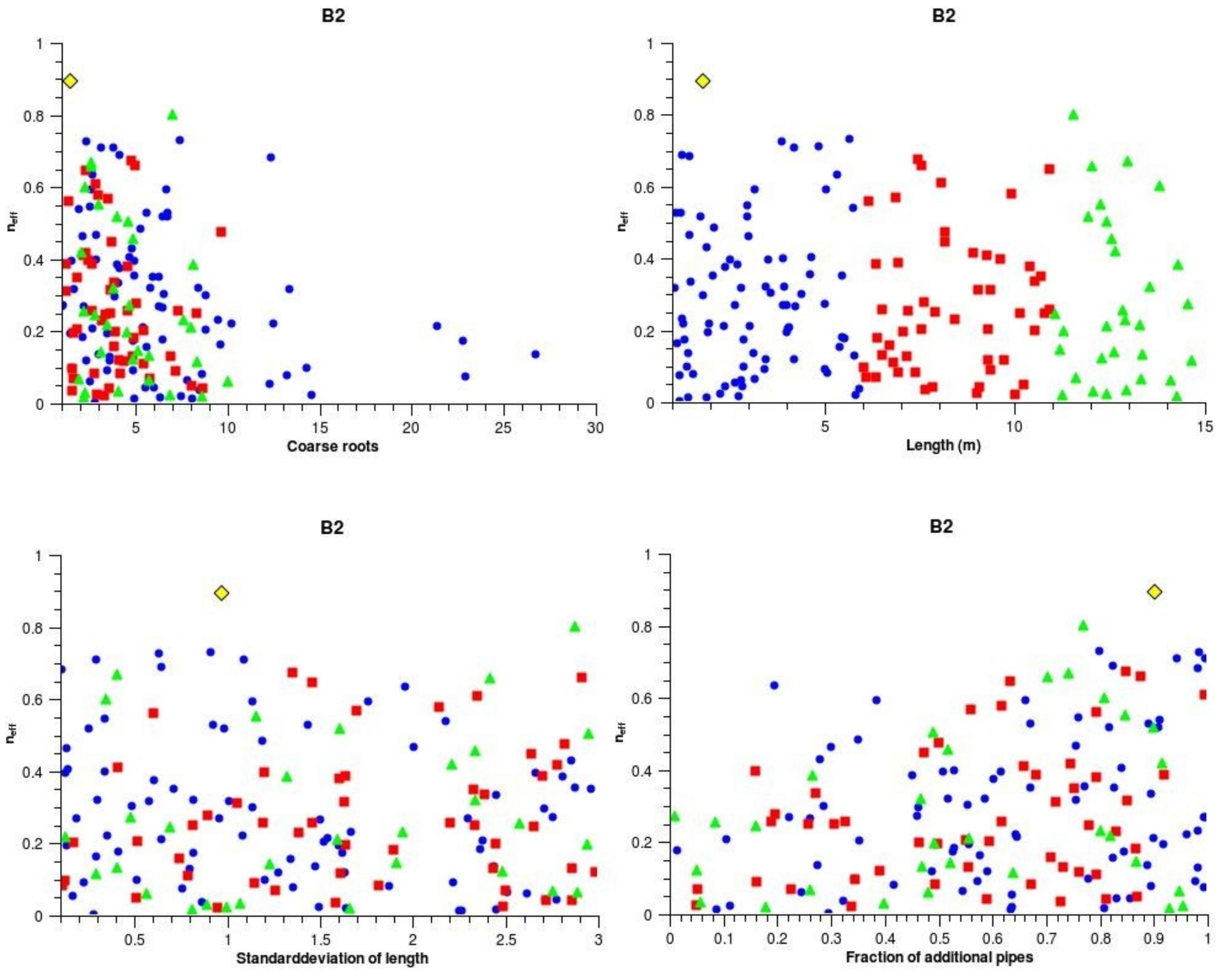

Figure 31: Variation of root parameters for plot B2 with root length classified.
Blue is length from 1 to 5, red from 6 to 10 and green from 11 to 15. Best values are represented by yellow diamonds.

The division of the coarse root number into classes depicted in Figure 30 shows that the sets with more roots per tree result into shorter roots with low standard deviation and a high fraction of additional pipes. The sets with fewer roots distribute rather homogeneous over the range, but also show the overall tendency toward high fractions of additional pipes.

The division of the root length into classes depicted in Figure 31 verifies this observations, since all sets with higher values for coarse root numbers come from the lowest length-class. For the standard deviation of length the values from all classes distribute homogeneous, only the short roots showing a tendency towards low values. Again, all classes tend to a high fractions of additional pipes.

Table 10: Best values for the calibration with root parameters.

	B2	S2
Efficiency	0.895	0.955
Number of coarse roots	1	8
Root length (m)	1.804	1.034
Standard deviation of length	0.970	2.831
Fraction of additional pipes	0.902	0.988

The calibration of S2, depicted in Figure 32 and Figure 33, resulted in far more parameter sets with efficiencies above 0 than the calibration of B2. Also the vast number of sets distributes all in all quite homogeneous. If any, there is a slight tendency towards low values for coarse roots.

Similar to B2, the best value for the number of coarse roots is below 10 and the best value for root length is around 1.

The value for standard deviation is a higher than for B2 and lies on the opposite end of the range.

The best value for the fraction of additional pipes is also very high.

Figure 32 shows the classing of coarse roots. Similar to the general trend the classes are evenly distributed over the parameter ranges. Only the classes with higher values for coarse roots have a slight tendency towards lower values of root length. Another remarkable feature is, that again the blue dots, which resemble the sets with low values for coarse root numbers, dominate the higher efficiencies. The dominance is not as sole as for the beech-plot, but nevertheless existent.

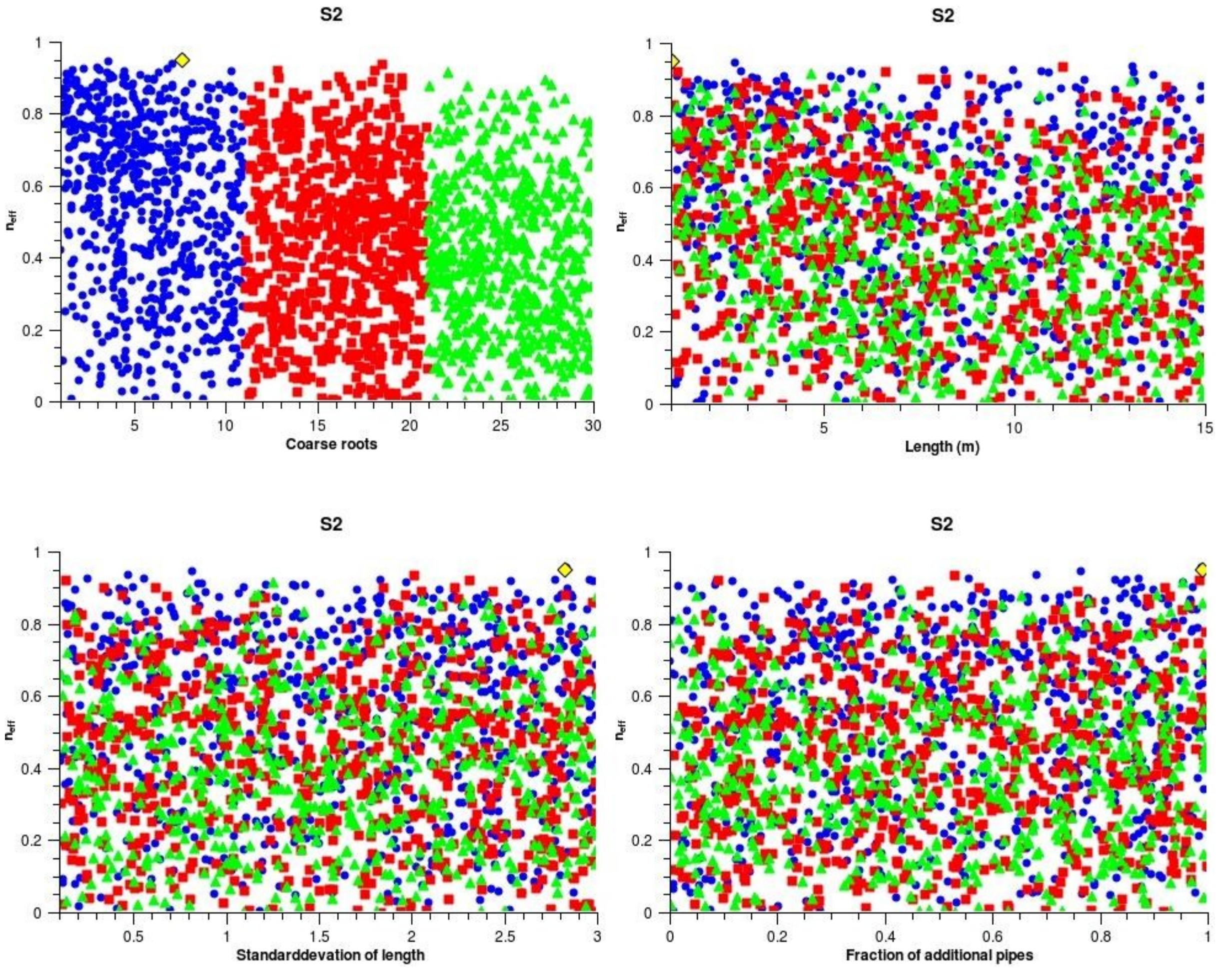

Figure 32: Variation of root parameters for plot S2 with coarse root number classified.
Blue is coarse root number from 1 to 10, red from 11 to 20 and green from 21 to 30. Best values are represented by yellow diamonds.

Figure 33 shows the division into classes for the root length. Again, the classes are more or less evenly distributed over the ranges. Only remarkable features, if any, is a slight dominance of short roots and a crowding of high values for root length in the lowest third of the coarse root range.

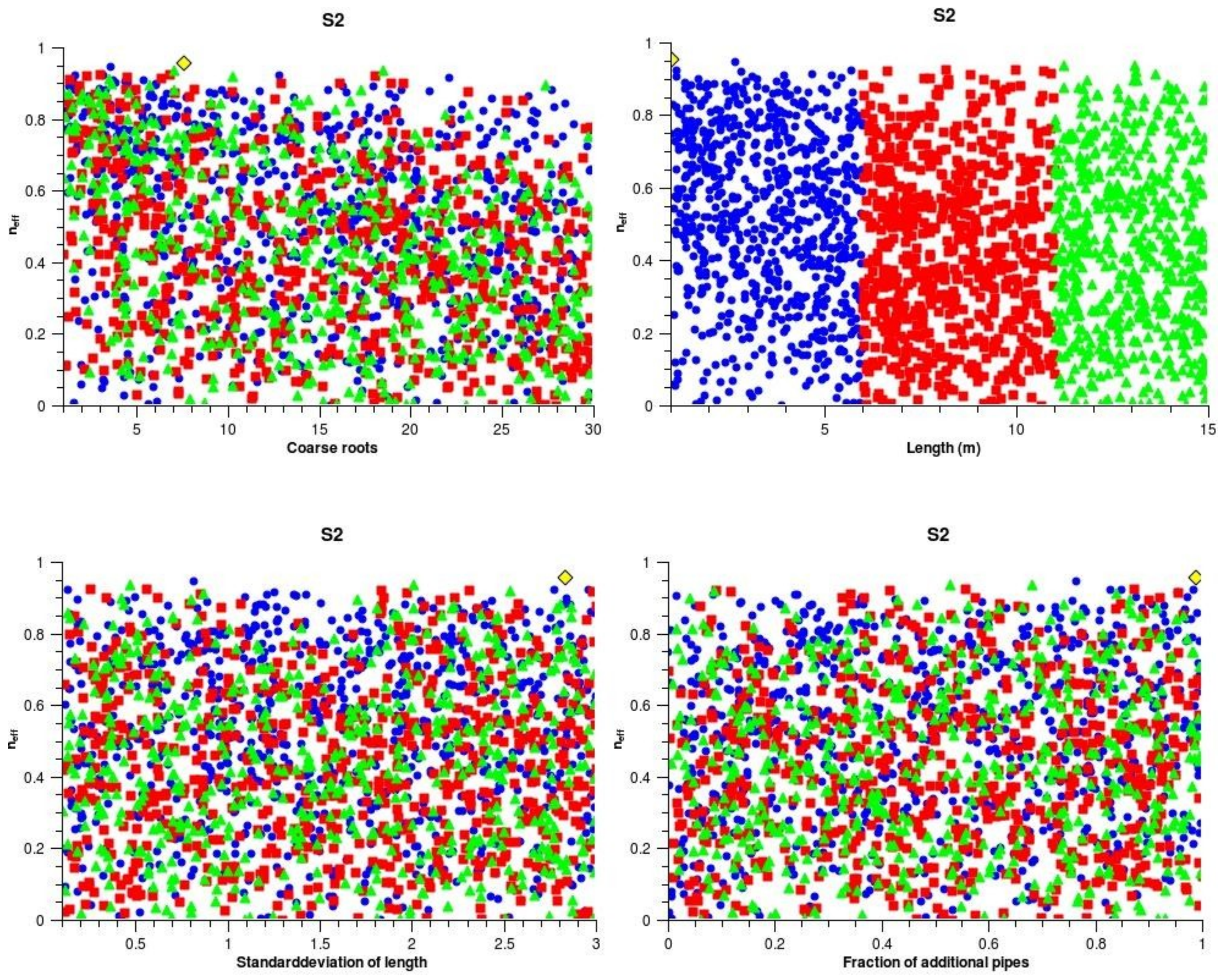

Figure 33: Variation of root parameters for plot S2 with root length classified.

Blue is length from 1 to 5, red from 6 to 10 and green from 11 to 15. Best values are represented by yellow diamonds.

7. Discussion

In the following the results presented above are discussed in respect to the reasons for the given behavior of the modelings and to the influence of the results on the relevance of root parameters.

7.1. Calibration without additional pipes

As mentioned above the results for the first calibration were surprisingly good. Efficiencies above 0.7 were considered to be acceptable, even if in total just a few runs reached values above 0. But observing model behavior and processes in animations during modeling, and comparing the runoff components modeled afterwards showed, that a significant part of the runoff was generated by overland flow. Both Jost (2004) and Nordmann et al. (2009) explicitly state, that in forestal catchments in these climates no surface runoff can be expected, what thoroughly can be called common sense, and that no overland flow was observed. As a result, the model concept used can not be right, or should be considered as right for the wrong reasons.

So, why is that? The primary reason is the root structure used itself.

Once again looking at the exemplary Figure 11, it shows us a dead-end root in the upper part of the plot. Water that is transported along a root is, in an optimal way, routed down a self organizing downhill way by activating more and more intersecting root parts. Finally the water reaches an exit, here the trench or the edge of the plot, and no water is backed up. That would be the optimum. But in a major fraction of the modelings one or more dead-end root occur. That means that a downhill oriented root ends in a cell where no other roots intersect. For the water, which comes along this root and spills into the final cell, the only remaining possibility is to be transported by matrix flow. It is obvious that matrix flow, that in general has a by magnitudes smaller transport capacity than pipe flow, is not able to handle the incoming water. That leads to saturation and, in the model, to overland flow.

Another process linked to root geometry leading to a comparable effect is the model's analogy to the double funneling effect described by Liang et al. (2007). The setting in the lower part of the slope in Figure 11 and around the tree positions in Figure 12 visualize this effect: Some roots with seemingly high transport capacities converge on a tree. The result is saturation in the area around the tree. If there now are less roots downslope than upslope or the downslope roots do not have sufficient capacities to cope with the incoming water, overland flow is generated. In nature this process has an influence on soil moisture patterns of forest soils. But still overland flow is not considered to occur in nature, since especially the soils in the area directly around a tree have very high conductivities due to fine roots (compare Figure 4 and Chandler & Chappell (2008)).

A further issue of the root system is an issue of stochastic positioning. While positioning trees as well as roots by stochastic means it is highly likely, that just few or even no roots end up in the trench. Preferential flow along roots then is not registered by the model.

The secondary reason is the general structure of the model. To provide sufficient capacity to transport incoming water only with matrix flow, the conductivities in cells with no pipe would need to be higher than in cells with a root. Concerning forests the situation in nature would rather be the other way round: Where a coarse root is, soils tend to be more conductive, due to the fine roots growing out of the coarse root.

To sum this issue up, the number of pipes just seems not to be sufficient for transport.

Anyway, Figure 12 shows in a better resolution how the root systems generated could look like. Comparing this to Figure 6 the basic method of root system generation still might be considered as good.

7.2. Calibration with additional pipes

Due to the fact that the pipe system is not sufficient, the other extremity was tried, putting in the maximum amount of additional pipes.

Again this resulted in very good efficiencies above 0.8 or even 0.9.

Parameters calibrated showed in general rather low sensitivities, resulting in more or less evenly distributed sets over the whole range. This softens the fact, that some physical parameters calibrated did not agree with the measurements. Total porosity, for example, was measured 0.54 by Schume et al. (2004) for the plots in Kreisbach catchment (compare Table 1). S1 and B2 calibrated to 0.47 and 0.48 respectively, and B1 to 0.52, which is a little closer. But for the plots mentioned efficiencies for total porosity of around 0.54 are still 0.7 to 0.8.

In this context it is also remarkable, that, besides the hydraulic conductivity of the bedrock, the calibrated values for B1 and B2 differ, despite the fact that they are actually the same plot. This issue again is softened by the fact that most values behave rather insensitive.

Since B2 still reaches higher efficiencies than B1 and especially the initial moisture content calibrates to a value around field capacity for this soil, it should be considered to calibrate the water table in general, which here was just done for B2.

All in all just a small part of the calibrations reached efficiencies above 0, even if significantly more frequent than without additional pipes. For beech it were usually around 300 to 500. For spruce less. In general, this actually is related to the same reasons as mentioned in the previous chapter. Especially the double funneling effect also occurred in model designs with additional pipes and generated overland flow. Also there was a lack of connectivity from roots to additional pipes. For example, a root that moves laterally through a cell marks the cell as containing a pipe and is ignored by the routine that positions additional pipes. This results in gaps between pipe networks, inhibiting pipe flow if not even generating overland flow, and very low efficiencies.

The even worse results for spruce relate to the higher root length compared to beech. Longer roots mean a bigger chance to reach the edge of a plot and to spill out. This results in to high mass deficits and low efficiencies. Still this process is considered important, since the experimentalist deems it as crucial for mass balances in sprinkling experiments.

7.3. Validation

The plots not calibrated yet were used to validate the models. The original plan was to gain a single parameter set for each tree species for validation. But since the parameter sets differed to much the validation was made with each parameter set.

In all cases the model was not capable to resemble the first observed runoff reaction. One reason could be the high weight of the model on pipe flow. The maximum depth of the beech roots was set to 0.7 meters, for spruce to 0.6 meters. Jost (2004) mentions, that after the metal sheet installed in the trench face of the beech-plot was pushed out by water pressure, he observed a big part of the subsurface flow coming out at the topsoil-subsoil interface at around 0.6 meters depth. The first reaction of the measured hydrograph could result from flow due to transmissivity feedback or saturated flow on this interface. This process might not be sufficiently represented in the actual model.

The depth of the roots might also be the reason for the different reaction of the species to the third input from precipitation. Beech shows a tendency to rather react to early, which could relate to roots deeper in the soil.

In general the results for beech were better than for spruce. This might again be related to the processes described in the previous chapter, especially to root length. For the beech-plot the model was also capable to resemble the width of the hydrograph as well as the area below the hydrograph better. This again can relate to the fact, that for the shorter roots of beech it is less likely to generate a big mass deficit by exiting the plot.

The model overestimates the peaks in general and for the spruce-runs by a way higher factor than for the beech-runs. Again the different root lengths might be the answer. Once pipe flow is initiated, a spruce-root pointing to the trench can bridge longer distances in a direct line than a beech-root.

All in all it should be considered, that, despite the high Nash-Sutcliffe efficiencies for example of B3 with B2 data, the model shows poor performance by missing the first low peak and weighting the high peak to much. This is a general issue with these efficiencies (Schaefli & Gupta 2007).

7.4. Calibration of plot B3 and S3

The calibration of the plots used for validation was made to see if the efficiencies from validation could be beaten.

Surprisingly this was not the fact. On the contrary, the variation of the root geometries during the validation runs seemed to have a higher impact on model performance than the calibrated parameters themselves. This is a very interesting insight for the whole concept.

Emerging from this point, it would at least be interesting to test the effect of varying geometries and parameters for all plots with a very high number of Monte-Carlo runs and evaluate which spatial patterns in geometry lead to a higher model performance. It is likely that this just results in geometries which are technically of high performance but do not relate to nature in any way.

7.5. Variation of root parameters

The first remarkable feature from the calibration of the from root parameters is, that this time spruce has way more parameter sets with efficiencies above 0 than beech. The explanation for this might relate to plot size. B2 measures 5 to 10 meters, while S2 measures 5 to 20 meters. With this high number of Monte-Carlo runs it is likely that the geometries generated perform better on large plots, since high values for root length again might end in high mass deficits.

The optimal set for beech and its high efficiency shown in Table 10 leads to one conclusion: The model performs best on a small plot with the minimum number of roots, a low value for length with a standard deviation of 1, and a very high fraction of additional pipes. This setup could easily be represent by the model concept from Weiler & McDonnell (2007) and would not need other root parameters than the depth and density.

At the first sight the optimal sets for spruce do not have any clear tendencies. Still the best values for length and additional pipes are comparable to the results from the beech-plot.

8. Conclusion and outlook

The intention of this thesis was to evaluate the effect of pipe structures modeled with respect to the geometry of natural root systems on the prediction of subsurface flow in forested hillslopes.

To sum up the facts, root parameters could be used to the benefit of model performance. But the root parameters implemented here do not suffice. In the concept presented here the selection of the parameters from literature used to describe root geometry orientated on the concept presented by Weiler & McDonnell (2007). This means that the focus was on creating a system of single pipes by dividing the length of a root into parts, only defined by their height above the bedrock and the global pipe parameters. Physically this concept works out under certain conditions. But structurally the number of pipes derived this way do not suffice and model performance rises the closer the pipe geometry comes to randomly placed pipes.

One option now would be to determine further parameters describing root systems to simply increase the number of pipes and to guarantee that all areas are sufficiently drained. Drexhage (1994) for example presents a concept to parametrize the branching of roots. Therefore he classifies the branching patterns observed in nature by the angle of branching and the number of branches in relation to root length. Even if there is few concrete data on this parameter in literature it could easily be implemented into a root model. In the course of this tortuosity of roots could be implemented, too (compare Figure 6).

The other option would be to improve the knowledge about the density of pipes initiated by roots and the mean height of roots above bedrock including a standard deviation by demanding more reliable data from experimentalists. A possible concept would be to develop spatial patterns of pipe density related to the distance between trees, similar to kriging.

Literature also showed other opportunities to simplify model parametrization by root information, besides preferential flow. One possibility could be to relate soil stratification and root intensity to hydraulic conductivity. Efforts to test this were already made (Chandler & Chappell 2008). Another idea is to implement bypass flow along a taproot supplied by stem flow (Lange et al. 2008).

All concepts would need further quantification by the forestal sciences.

9. References

Aubertin, G. M. (1971): *Macropores in forest soils*, U.S.D.A. Forest research papers 192, pp. 33.

Beven, K. & Germann, P. (1982): *Macropores and water flow in soils*, Water Resources Research 18, pp. 1311-1325.

Bonell, M. (1993): *Progress in the understanding of runoff generation dynamics in forests*, Journal of Hydrology 150, pp. 217-275.

Chandler, K. R. & Chappell, N. A. (2008): *Influence of individual oak (Quercus robur) trees on saturated hydraulic conductivity*, Forest Ecology and Management 256, pp. 1222-1229.

Devitt, D. A. & Smith, S. D. (2002): *Root channel macropores enhance downward movement of water in a Mojave Desert ecosystem*, Journal of arid environment 50, pp. 99-108.

Drexhage, M., (1994): *Die Wurzelentwicklung 40-jähriger Fichten (Picea abies [L.] Karst.) in der Langen Bramke (Harz)*, Selbstverlag des Forschungszentrums Waldökosysteme der Univarsität Göttingen, 165 pp.

Faeh, A. (1997). *Understanding the processes of discharge formation under extreme precipitation, A study based on the numerical simulation of hillslope experiments*, Eidgenössische Technische Hochschule.

Fogel, R. (1983): *Root turnover and productivity of coniferous forests*, Plant and Soil 71, pp. 75-85.

Freeze, A. R. & Cherry, J. A. (1979): *Groundwater*, Prentice Hall, 604 pp.

von Gadow, K. (2003): *Waldstruktur und Wachstum*, Universitätsverlag Göttingen, 241 pp.

Gish, T. J.; Gimenez, D. & Rawls, W. J. (1998): *Impact of roots on ground water quality*, Plant and Soil 200, pp. 47-54.

Hagedorn, F. & Bundt, M. (2002): *The age of preferential flow paths*, Geoderma 108, pp. 119-132.

Hilf, H. H. (1927). *Studien über die Wurzelausbreitung von Fichte, Buche und Kiefer in geschlossenern älteren Beständen, insbesondere auf Sandböden*, Eberswalde.

Holden, J. (2005): *Piping and woody plants in peatlands: Cause or effect?*, Water Resources Research 41.

Johnson, M. & Lehmann, J. (2006): *Double funneling of trees; Stemflow and root-induced preferential flow*, Ecoscience 13, pp. 324-333.

Jorgensen, P. R.; Hoffmann, M.; Kistrup, J. P.; Bryde, C.; Bossi, R. & Villholth, G. G. (2002): *Preferential flow and pesticide transport in a clay-rich till: Field, laboratory and modelling analysis*, Water Resources Research 38, pp. 1246.

Jost, G. (2004): *Analyse der Wassergehaltsänderungen und der Abflussprozesse im Wurzelraum von Waldbeständen - Dynamics of soil water content and flow processes in the rooting zone of forest stands*, Universität für Bodenkultur Wien.

Kalinin, M., (1983): *Ausbildung der Wurzelsysteme von Bäumen (russ.)*, Lesnaja Promyschlennost, Moskwa, 151 pp.

Kirchner, J. W. (2003): *A double paradox in catchment hydrology and geochemistry*, Hydrological Processes 17, pp. 871-874.

Kuhr, M. (1999). *Grobwurzelarchitektur in Abhängigkeit von Baumart, Alter, Standort und sozialer Stellung*, Georg-August-Universität Göttingen.

Köstler, J. N., (1968): *Die Wurzeln der Waldbäume*, Paul Parey Verlag, Hamburg, 284 pp.

Lange, B.; Luescher, P. & Germann, P. F. (2008): *Significance of tree roots for preferential infiltration in stagnic soils*, Hydrology and Earth System Sciences Discussions 5, pp. 2373-2407.

Liang, W.; Kosugi, K. & Mizuyama, T. (2007): *Heterogeneous soil water dynamics around a tree growing on a steep hillslope*, Vadose Zone Journal 6, pp. 879-889.

Lüscher, P. & Zürcher, K. (2002): *Wald schützt nicht immer vor Hochwasser*, Informationsblatt Forschungsbereich Wald 9, pp. 1-2.

McDonnell, J. (1990): *A rationale for old water discharge through macropores in a steep, humid catchment*, Water Resources Research 26, pp. 2821–2832.

McGuire, K.; Weiler, M. & McDonnell, J. (2007): *Integrating tracer experiments with modeling to assess runoff processes and water transit times*, Advances in Water Resources 30, pp. 824-837.

van Meerveld, H. J. T. & McDonnell, J. J. (2006): *Threshold relations in subsurface stormflow: 1. A 147-storm analysis of the Panola hillslope*, Water Resources Research 42, pp. 11.

van Meerveld, I. T. & Weiler, M. (2008): *Hillslope dynamics modeled with increasing complexity*, Journal of Hydrology 361, pp. 24-40.

Mitchell, A. R.; Ellsworth, T. R. & Meek, B. D. (1995): *Effect of root systems on preferential flow in swelling soil*, Commun. Soil Sci. Plant Anal. 26, pp. 2655-2666.

Nash, J. & Sutcliffe, J. (1970): *River flow forecasting through conceptual models part I: A discussion of principles*, Journal of Hydrology 10, pp. 282-290.

Nieber, J. L. & Warner, G. S. (1991): *Soil pipe contribution to steady subsurface stormflow*, Hydrological Processes 5, pp. 329-344.

Noguchi, S.; Tsuboyama, Y.; Sidle, R. C. & Hosoda, I. (1999): *Morphological Characteristics of Macropores and the Distribution of Preferential Flow Pathways in a Forested Slope Segment*, Soil Science Society of America Journal 63, pp. 1413-1423.

Nordmann, B.; Göttlein, A. & Binder, F. (2009): *Einfluss unterschiedlicher Waldbestockung auf die Abflussbildung – ein Beispiel aus einem Wassereinzugsgebiet im Frankenwald*, Hydrologie und Wasserbewirtschaftung 53, pp. 80-95.

Oswald, S. E.; Menon, M.; Carminati, A.; Vontobel, P.; Lehmann, E. & Schulin, R. (2008): *Quantitative imaging of infiltration, root growth, and root water uptake via neutron radiography*, Vadose Zone Journal 7, pp. 1035–1047.

Perillo, C.; Gupta, S.; Nater, E. & Moncrief, J. (1999): *Prevalence and initiation of preferential flow paths in a sandy loam with argillic horizon*, Geoderma 89, pp. 307-331.

Polomski, J. & Kuhn, N. (1998): *Wurzelsysteme*, Eidgenössische Forschungsanstalt für Wald, Schnee und Landschaft, Birmensdorf, 290 pp.

Rupp, D. E. & Selker, J. S. (2005): *Drainage of a horizontal Boussinesq aquifer with a power law hydraulic conductivity profile*, Water Resources Research 41, pp. 8.

Schaefli, B. & Gupta, H. V. (2007): *Do nash values have value?*, Hydrological Processes 21, pp. 2075-2080.

Scheffer, F. & Schachtschabel, P. (2002): *Lehrbuch der Bodenkunde*, 15. edition, Spektrum Akademischer Verlag, Heidelberg, 593 pp.

Schume, H.; Jost, G. & Hager, H. (2004): *Soil water depletion and recharge patterns in mixed and pure forest stands of European beech and Norway spruce*, Journal of Hydrology 289, pp. 258-274.

Seibert, J. & McDonnell, J. J. (2002): *On the dialog between experimentalist and modeler in catchment hydrology: Use of soft data for multicriteria model calibration*, Water Resources Research 38, pp. 14.

Sidle, R. C.; Kitahara, H.; Terajima, T. & Nakai, Y. (1995): *Experimental studies on the effects of pipeflow on throughflow partitioning*, Journal of Hydrology 165, pp. 207-219.

Sidle, R. C.; Noguchi, S.; Tsuboyama, Y. & Laursen, K. (2001): *A conceptual model of preferential flow systems in forested hillslopes: evidence of self-organization*, Hydrological Processes 15, pp. 1675-1692.

Sponagel, H., (2005): *Bodenkundliche Kartieranleitung*, 5. edition, Ad-hoc-Arbeitsgruppe Boden, Bundesanstalt für Geowissenschaften und Rohstoffe in Zusammenarbeit mit den Staatlichen Geologischen Diensten, Hannover, 438 pp.

Uchida, T.; Kosugi, K. & Mizuyama, T. (2001): *Effects of pipeflow on hydrological process and its relation to landslide: a review of pipeflow studies in forested headwater catchments*, Hydrological Processes 15, pp. 2151-2174.

Uchida, T.; van Meerveld, I. T. & McDonnell, J. J. (2005): *The role of lateral pipe flow in hillslope runoff response: an intercomparison of non-linear hillslope response*, Journal of Hydrology 311, pp. 117-133.

Weiler, A.; McDonnell, J.; van Meerveld, I. T. & Uchida, T. (2005): *Subsurface Stormflow*, Encylopedia of Hydrological Sciences 10, pp. 14.

Weiler, M. (2005): *An infiltration model based on flow variability in macropores: development, sensitivity analysis and applications*, Journal of Hydrology 310, pp. 294-315.

Weiler, M. & McDonnell, J. (2004): *Virtual experiments: a new approach for improving process conceptualization in hillslope hydrology*, Journal of Hydrology 285, pp. 3-18.

Weiler, M. & McDonnell, J. J. (2006): *Testing nutrient flushing hypotheses at the hillslope scale: A virtual experiment approach*, Journal of Hydrology 319, pp. 339-356.

Weiler, M. & McDonnell, J. J. (2007): *Conceptualizing lateral preferential flow and flow networks and simulating the effects on gauged and ungauged hillslopes*, Water Resources Research 43, pp. 13.

Weiler, M.; Uchida, T. & McDonnell, J. (2003): *Connectivity due to preferential flow controls water flow and solute transport at the hillslope scale*. In: MODSIM 2003, Townsville, Queensland, Australia, 6 pp.

Wigmosta, M. S. & Lettenmaier, D. P. (1999): *A Comparison of Simplified Methods for Routing Topographically Driven Subsurface Flow*, Water Resources Research 35, pp. 255-264.